ChemInform Abstract: Synthesis, Biological Evaluation, and Pharmacophore Generation of New Pyridazinone Derivatives with Affinity Toward α1- and α2-Adrenoceptors.

ARTICLE *in* JOURNAL OF MEDICINAL CHEMISTRY · JULY 2001

Impact Factor: 5.45 · DOI: 10.1021/jm010821u · Source: PubMed

9 AUTHORS, INCLUDING:

Laura Betti
Università di Pisa
117 PUBLICATIONS **1,198** CITATIONS
SEE PROFILE

Federico Corelli
Università degli Studi di Siena
236 PUBLICATIONS **2,986** CITATIONS
SEE PROFILE

Laura Maccari
24 PUBLICATIONS **431** CITATIONS
SEE PROFILE

Synthesis, Biological Evaluation, and Pharmacophore Generation of New Pyridazinone Derivatives with Affinity toward α_1- and α_2-Adrenoceptors[1]

Roberta Barbaro,[†] Laura Betti,[‡] Maurizio Botta,*[,§] Federico Corelli,[§] Gino Giannaccini,[‡] Laura Maccari,[§] Fabrizio Manetti,[§] Giovannella Strappaghetti,*[,†] and Stefano Corsano[†]

Istituto di Chimica e Tecnologia del Farmaco, Università di Perugia, Via del Liceo 1, 06123 Perugia, Italy, Dipartimento di Psichiatria, Neurobiologia, Farmacologia e Biotecnologie, Università di Pisa, Via Bonanno 6, 56126 Pisa, Italy, and Dipartimento Farmaco Chimico Tecnologico, Università degli Studi di Siena, Via Aldo Moro, 53100 Siena, Italy

Received January 15, 2001

A series of new pyridazin-3(2*H*)-one derivatives (**3** and **4**) were evaluated for their in vitro affinity toward both α_1- and α_2-adrenoceptors by radioligand receptor binding assays. All target compounds showed good affinities for the α_1-adrenoceptor, with K_i values in the low nanomolar range. The polymethylene chain constituting the spacer between the furoylpiperazinyl pyridazinone and the arylpiperazine moiety was shown to influence the affinity and selectivity of these compounds. Particularly, a gradual increase in affinity was observed by lengthening the polymethylene chain up to a maximum of seven carbon atoms. In addition, compound **3k**, characterized by a very interesting α_1-AR affinity (1.9 nM), was also shown to be a highly selective α_1-AR antagonist, the affinity ratio for α_2- and α_1-adrenoceptors being 274. To gain insight into the structural features required for α_1 antagonist activity, the pyridazinone derivatives were submitted to a pharmacophore generation procedure using the program Catalyst. The resulting pharmacophore model showed high correlation and predictive power. It also rationalized the relationships between structural properties and biological data of, and external to, the pyridazinone class.

Introduction

The α_1- and α_2-adrenoceptors (termed α_1-AR and α_2-AR, respectively, in the text) are members of the seven-transmembrane-spanning domain group sharing the common structural motif of seven putative α-helical segments traversing the cell membrane.

It is now clear that α_1-ARs are comprised of multiple subtypes that have been identified by both pharmacological and binding studies. To date, they are classified into α_{1A}, α_{1B}, and α_{1D}[2] and the corresponding cloned counterparts termed α_{1a}-, α_{1b}-, and α_{1d}-AR, respectively.[3] In addition, the existence of an additional subtype (α_{1L}), characterized by a low affinity for prazosin, has been postulated.

In a similar way, α_2-ARs have been classified into four subtypes, called α_{2A}−α_{2D}, respectively.[2c]

In recent years, the search for new selective α_1-AR antagonists has intensified, due to their importance in the treatment of hypertension and of benign prostatic hyperplasia (BPH). In fact, α_1-AR blockers have been employed in the treatment of BPH for more than two decades, due to the significant improvements in symptoms and flow rates in patients with bladder outflow obstruction.[4,5] Nevertheless, the efficacy of α_1-AR antagonists in the treatment of BPH is balanced against a small, but significant, incidence of side effects, such as orthostatic hypotension, which is considered a critical disadvantage in BPH patients. On the other hand, some of these effects, such as a significant reduction of both systolic and diastolic blood pressure in hypertensive patients,[6] and the favorable reduction in the level of LDL cholesterol as well as serum triglyceride profiles,[7] could be construed as beneficial.

Molecular cloning studies[8,9] have shown that the α_1- and α_2-adrenoceptors have many common features which could reflect their similar mechanisms of action. As a consequence of such similarities, synthetic compounds with affinity toward α-AR are expected to potentially bind to both α_1 and α_2 receptors. On the other hand, many literature reports revealed that the addition of arylpiperazinylalkyl side chains into different heterocycles, like uracils or the pyrimido[5,4-*b*]-indole moiety,[10] provides compounds that effectively lower blood pressure by antagonizing the α_1-AR. Moreover, great attention has been paid to the compounds containing a pyridazin-3(2*H*)-one moiety, due to their potential biological activities as antihypertensive agents (compound GYKI-12743 is an example).[11] This literature survey led to the suggestion that both the arylpiperazinyl and the pyridazinone moiety are key elements for α_1-AR affinity.

On the basis of this experimental evidence, in the course of our studies in the field of new and potentially selective α_1-AR antagonists containing a pyridazin-3(2*H*)-one ring, we have recently synthesized compounds **1** and **2**[12] (Figure 1 and Table 1) bearing an arylpiperazinylalkyl chain at the 2-position of the pyridazinone moiety. While they all exhibited a good affinity toward α_1-AR, with values ranging from 0.6

* To whom correspondence should be addressed. M.B.: Dipartimento Farmaco Chimico Tecnologico, Università degli Studi di Siena, Via Aldo Moro, I-53100 Siena, Italy; telephone, +39 0577 234306; fax, +39 0577 234333; e-mail, botta@unisi.it. G.S.: Istituto di Chimica e Tecnologia del Farmaco, Università di Perugia, Via del Liceo 1, I-06123 Perugia, Italy; telephone, +39 075 5855136; fax, +39 075 5855129; e-mail, noemi@unipg.it.

[†] Università di Perugia.

[‡] Università di Pisa.

[§] Università degli Studi di Siena.

10.1021/jm010821u CCC: $20.00
Published on Web 05/26/2001

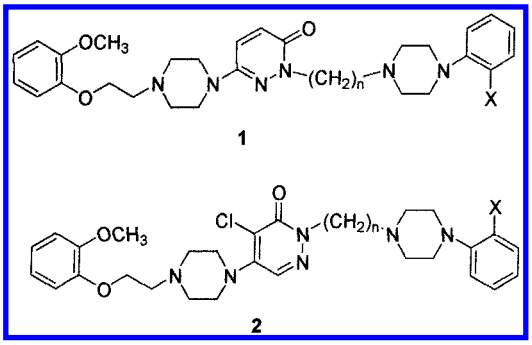

Figure 1. General structures of compounds **1** and **2**.

Table 1. α_1- and α_2-Adrenergic Receptor Binding Affinities for Pyridazin-3(2*H*)-one Derivatives **1** and **2**

			K_i[a] (nM)		
compd	*n*	X	α_1-AR[b]	α_2-AR	α_2/α_1
1a	2	OCH_3	38.0 ± 5.0	1261.0 ± 210.0	33.2
1b	3	OCH_3	7.3 ± 0.6	254.0 ± 40.3	34.8
1c[c]	4	OCH_3	0.6 ± 0.1 (1.8)	62.0 ± 8.0	103.3
1d	5	OCH_3	12.9 ± 1.5	69.8 ± 9.2	5.4
1e	6	OCH_3	7.0 ± 0.8	71.8 ± 6.3	10.2
1f[d]	7	OCH_3	2.3 ± 0.2 (19)	45.8 ± 6.3	20.0
1g	2	Cl	18.0 ± 2.0	370.0 ± 50.2	20.5
1h[c]	3	Cl	6.8 ± 0.6 (7.5)	316.0 ± 40.3	46.5
1i[c]	4	Cl	0.8 ± 0.1 (3.3)	69.4 ± 6.0	86.7
1j	5	Cl	7.0 ± 0.9	138.0 ± 25.0	20.0
1k	6	Cl	8.4 ± 1.2	138.8 ± 20.3	16.5
1l	7	Cl	15.0 ± 2.5	139.0 ± 15.3	9.3
2a	2	OCH_3	16.0 ± 1.7	409.0 ± 35.7	25.5
2b[c]	3	OCH_3	14.5 ± 1.3 (4.9)	245.0 ± 25.3	17.0
2c	4	OCH_3	4.3 ± 0.3	230.0 ± 20.0	53.0
2d	5	OCH_3	3.9 ± 0.2	15.0 ± 1.9	3.8
2e[d]	6	OCH_3	1.5 ± 0.1 (14)	3.5 ± 0.4	2.3
2f[c]	7	OCH_3	1.4 ± 0.1 (9.7)	4.6 ± 0.5	3.2
2g	8	OCH_3	3.5 ± 0.4	22.7 ± 3.0	6.5
2h[c]	2	Cl	58.8 ± 3.7 (39)	292.3 ± 30.2	5.0
2i[d]	3	Cl	27.8 ± 3.0 (5.6)	219.0 ± 15.8	7.8
2j[d]	4	Cl	10.0 ± 1.5 (2.8)	39.3 ± 5.3	4.0
2k[c]	5	Cl	4.5 ± 0.2 (8.6)	29.0 ± 4.5	6.4
2l	6	Cl	4.2 ± 0.6	25.2 ± 3.8	6.0
2m	7	Cl	2.7 ± 0.3	7.4 ± 0.5	2.7
2n	8	Cl	5.6 ± 0.7	22.8 ± 2.5	4.0
prazosin			0.24 ± 0.05		
rauwolscine				4.0 ± 0.3	

[a] The K_i binding data were calculated as described in the Experimental Section. The K_i values are means ± standard deviation (SD) of separate series assays, each performed in triplicate. Inhibition constants (K_i) were calculated according to the equation of Cheng and Prusoff:[36] $K_i = IC_{50}/[1 + ([L]/K_d)]$, where [L] is the ligand concentration and K_d its dissociation constant. The K_d of [^{3}H]prazosin binding to rat cortex membranes was 0.24 nM (α_1), and the K_d of [^{3}H]rauwolscine binding to rat cortex membranes was 4 nM (α_2). [b] In parentheses are estimated and predicted affinity values calculated by Catalyst for the training set and test set, respectively. [c] Compounds used to build the training set. [d] Compounds used to build the test set.

(compound **1c**) to 58.8 nM (compound **2h**), a good selectivity was found for compound **1i** [α_2/α_1 ratio of 86.7 (Table 1)] and **1c** [α_2/α_1 ratio of 103.3 (Table 1)].

The goal of this work was the synthesis of new pyridazinone derivatives possibly characterized by high affinity and selectivity toward the α_1-adrenoceptors. In this paper, we report the synthesis and biological evaluation of pyridazinone derivatives **3** and **4** (Scheme 1 and Table 2) bearing at the 2-position an ortho-substituted arylpiperazinylalkyl side chain and, at the 5- or 6-position, a furoylpiperazinyl moiety. In addition, taking into account the fact that the new pyridazinones showed a higher affinity toward α_1-AR than toward α_2-AR, to investigate the structure−affinity relationships of these ligands, we have used the program Catalyst[13] to develop a pharmacophore model for α_1-AR antagonists. The calculated model, able to rationalize the relationships between the chemical features of new structures **3** and **4** and their binding affinity data at α_1-AR, consists of a positive ionizable portion, three hydrophobic features, and a hydrogen bond acceptor group. It shows a good statistical significance ($r = 0.92$, rmsd = 0.89) and successfully predicts the affinities of the molecules of, and external to, the training set.

Chemistry

The target compounds **3** and **4** listed in Table 2 were synthesized as outlined in Scheme 1. The first series of compounds **3** were prepared starting from 4-chloro-5-[4-(2-furoyl)piperazin-1-yl]pyridazin-3(2*H*)-one (**5**), obtained by condensation of 4,5-dichloropyridazin-3(2*H*)-one and 1-(2-furoyl)piperazine in DMF and potassium carbonate or EtOH and Et_3N according to the procedure reported by Gòmez-Gil.[14]

Alkylation of **5** with 1-(2-methoxyphenyl)-4-(3-chloropropyl)piperazine (**6a**)[15] or 1-(2-chlorophenyl)-4-(3-chloropropyl)piperazine (**6b**)[15] in dry ethanol in the presence of sodium hydroxide (method A) afforded compounds **3a** and **3b**, respectively, in moderate yield. Alternatively, **5** was alkylated with 1,2-dibromoethane under phase transfer catalysis, according to the procedure reported by Yamada,[16] to give intermediate **7a**, which in turn was converted to final compounds **3c** and **3d** by reaction with 1-(2-methoxyphenyl)piperazine (**8**) or 1-(2-chlorophenyl)piperazine (**9**) (Na_2CO_3/isoamyl alcohol, method B) in 20−30% overall yield. α,ω-Dibromoalkanes having four to seven methylene groups were employed to prepare intermediates **7b**−**e** (K_2CO_3/acetone, method C), from which compounds **3e**−**l** were synthesized following method B. Analogously, compound **4d** was prepared by direct alkylation of **10**,[17] according to the procedure previously reported for the synthesis of **4a**−**c**,[17] while pyridazinones **4e**−**l** were obtained via intermediates **11a**−**d**, in turn prepared by treatment of **10** with dibromoalkanes (method C).

The chemical and physical data of the new compounds are reported in Table 3.

Molecular Modeling Studies

Pharmacophore Generation. Our goal is to gain insight into the structural factors responsible for α_1 affinity, and to design new ligands with possibly higher selectivity for the α_1 receptor, with respect to the α_2-AR. In particular, here we report a study that applies a ligand-based drug design (pharmacophore development) method to rationalize the relationships between new pyridazinone−arylpiperazine structures and their affinity data at the α_1 receptor. Experimentally determined affinities are used to derive a pharmacophore model that describes the three-dimensional structural properties required to have profitable interactions with α_1 receptor sites.

Since we were primarily interested in the design of new selective ligands for α_1-AR, based on pyridazinone−arylpiperazine lead compounds **1**−**4**, and various other molecules collected from the literature (Figure 2 and Table 4), we decided to employ a computational ap-

Scheme 1[a]

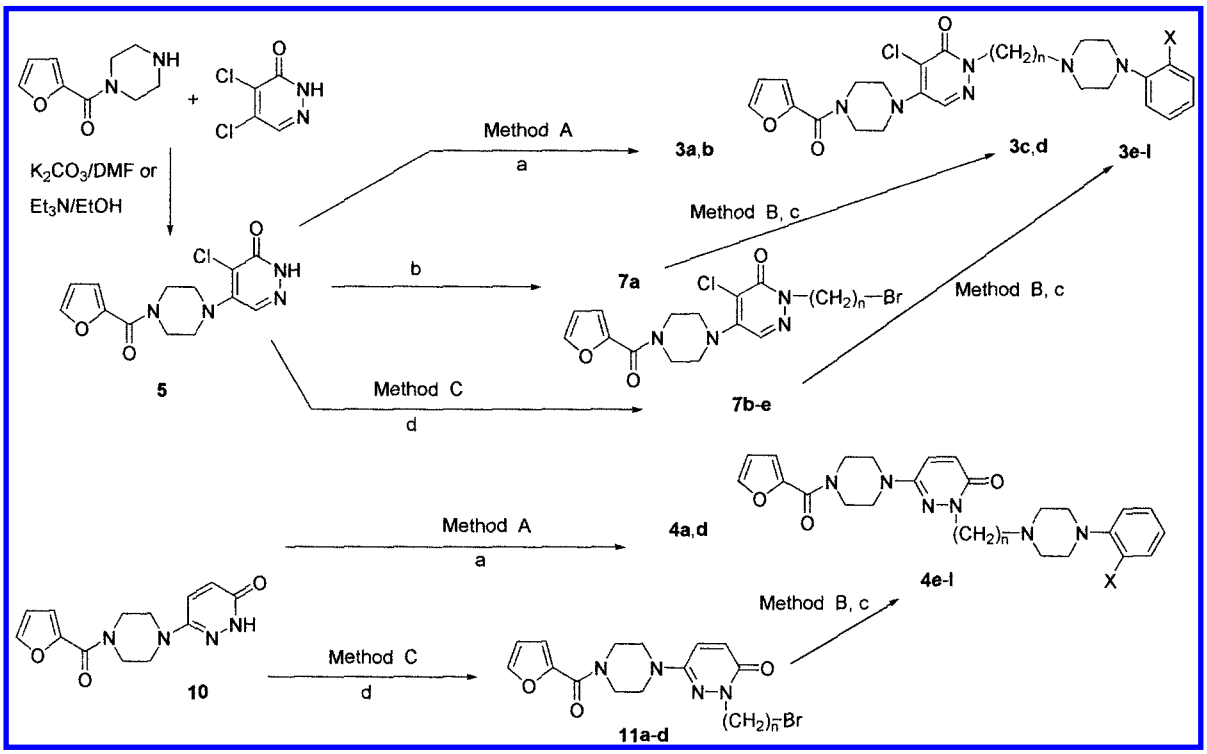

[a] Compounds: **3a**, $n = 3$, X = OCH_3; **3b**, $n = 3$, X = Cl; **3c**, $n = 2$, X = OCH_3; **3d**, $n = 2$, X = Cl; **3e**, $n = 4$, X = OCH_3; **3f**, $n = 4$, X = Cl; **3g**, $n = 5$, X = OCH_3; **3h**, $n = 5$, X = Cl; **3i**, $n = 6$, X = OCH_3; **3j**, $n = 6$, X = Cl; **3k**, $n = 7$, X = OCH_3; **3l**, $n = 7$, X = Cl; **4a**, $n = 2$, X = OCH_3; **4b**, $n = 2$, X = Cl; **4c**, $n = 3$, X = OCH_3; **4d**, $n = 3$, X = Cl; **4e**, $n = 4$, X = OCH_3; **4f**, $n = 4$, X = Cl; **4g**, $n = 5$, X = OCH_3; **4h**, $n = 5$, X = Cl; **4i**, $n = 6$, X = OCH_3; **4j**, $n = 6$, X = Cl; **4k**, $n = 7$, X = OCH_3; **4l**, $n = 7$, X = Cl; **7a**, $n = 2$; **7b**, $n = 4$; **7c**, $n = 5$; **7d**, $n = 6$; **7e**, $n = 7$; **11a**, $n = 4$; **11b**, $n = 5$; **11c**, $n = 6$; **11d**, $n = 7$. Reagents: (a) **6a** or **6b**, dry EtOH, NaOH; (b) $BrCH_2CH_2Br$, benzene, TBAB, KOH; (c) **8** or **9**, Na_2CO_3, isoamyl alcohol; (d) $Br(CH_2)_nBr$ ($n = 4-7$), K_2CO_3, acetone.

proach to build an "inclusive" pharmacophore for α_1-AR antagonists, without considering the additional variable of the selectivity between the α_1-AR subtypes. In fact, we provided the program with the structure of the compounds to be analyzed and their affinity data, without any information about the selectivity of the α_1-AR subtypes.

The training set for the pharmacophore development has been chosen according to the Catalyst guidelines.[18] Fourteen molecules of the whole set of pyridazinones (namely, compounds **1c**, **1h**, **1i**, **2b**, **2f**, **2h**, **2k**, **3e**, **3g**, **3l**, **4a**, **4e**, **4h**, and **4l**) have been selected as a part of the training set. They are characterized by affinity values spanning ~2.5 orders of magnitude, the minimum value of 0.6 nM being associated with compound **1c** and the maximum value of 184 nM being associated with compound **4e**. In addition, with the aim of covering the optimal value of 4 orders of magnitude in affinity required by the program, we investigated literature reports to find some additional α_1-AR antagonists with the appropriate biological properties. Within the large set of compounds that were found, to ensure the highest degree of homogeneity of biological data with respect to those of the pyridazinone derivatives, we have focused our attention on such compounds whose antagonist activity on α_1-AR was tested on rat cortex homogenates and expressed as K_i. Moreover, because we are mainly interested in compounds sharing common chemical features with pyridazinone derivatives **1**−**4**, we have decided to select only some of the arylpiperazine-bearing molecules found in the literature. Between them, para-substituted derivatives have not been arbitrarily included in the training set, taking into account the findings showing that para substituents (particularly, nitro and amino groups) are unfavorable to ligand−receptor binding. As an example, **12** [K_i = 0.21 nM (Figure 2)] has been reported to be much more active than its *p*-methoxy counterpart (K_i > 5000 nM).[10] Moreover, a CoMFA study[19] on hydantoin−phenylpiperazine derivatives has shown that the affinity of the para-substituted compounds is modulated mainly by steric factors. On the basis of this hypothesis, one may account for the dramatic drop in affinity observed when a nitro or amino group is introduced in the para position with respect to a fluoro substituent that leads to a moderate increase in affinity. In contrast, a different CoMFA study recently published[20] led to the conclusion that the para position is forbidden to electronegative substituents.

As a consequence of these choices, 10 additional compounds [namely, **12**−**15**, **18**, and **20**−**24** (Figure 2 and Table 4)] have been added to the training set to obtain a total number of 24 structures to be used for pharmacophore generation.

Biological data associated with the training set, expressed as K_i, were in the range between 0.21 (compound **12**) and 2396 nM (compound **13**). While the biological activities of compounds **1** and **2** (Table 1) and **3** and **4** (Table 2) were experimentally determined (see Experimental Section), data associated with the remaining compounds were assembled from the literature (Table 4) under the assumption that all these substances are acting through the same binding site.

Because no experimental data on the biologically

Table 2. α_1- and α_2-Adrenergic Receptor Binding Affinities for Pyridazin-3(2*H*)-one Derivatives **3** and **4**

	K_i[a] (nM)		
compd	α_1-AR[b]	α_2-AR	α_2/α_1
3a	20.4 ± 2.1	680.0 ± 120	33.3
3b[c]	3.5 ± 0.4 (11)	85.0 ± 18.3	24.3
3c[c]	33.0 ± 5.3 (36)	440.0 ± 36	13.3
3d	3.9 ± 0.2	150.0 ± 15.5	38.4
3e[d]	33.5 ± 4.7 (15)	870 ± 165	26.0
3f	19.0 ± 1.7	280.0 ± 38.5	14.7
3g[d]	1.9 ± 0.1 (10)	23.3 ± 3.2	12.3
3h	3.6 ± 0.3	18.0 ± 2.5	5.0
3i	4.1 ± 0.6	24.5 ± 3.6	6.0
3j	5.7 ± 0.5	66.0 ± 9.2	11.6
3k	1.9 ± 0.1	520.0 ± 4.2	273.7
3l[d]	11.5 ± 1.7 (19)	36.2 ± 5.3	3.1
4a[d,e]	94.5 ± 8.5 (31)	ND[f]	–
4b[e]	34.0 ± 5.3	52.6 ± 3.7	1.5
4c[e]	64.5 ± 5.7	631.0 ± 40.5	9.8
4d	12.8 ± 1.8	260.0 ± 24.5	20.3
4e[d]	180.0 ± 15.3 (88)	790.0 ± 54.3	4.4
4f[c]	7.9 ± 0.5 (10)	24.0 ± 3.8	3.0
4g	43.7 ± 5.2	255.0 ± 25.3	5.8
4h[d]	13.3 ± 1.2 (34)	105.0 ± 20.3	7.9
4i[c]	17.8 ± 2.5 (20)	100.0 ± 15.2	5.6
4j	5.9 ± 0.6	23.7 ± 2.5	4.0
4k	54.7 ± 6.7	96.0 ± 8.4	1.7
4l[d]	5.6 ± 0.5 (6.3)	23.5 ± 3.0	4.2
prazosin	0.24 ± 0.05		
rauwolscine		4.0 ± 0.3	

[a] The K_i binding data were calculated as described in the Experimental Section. The K_i values are means ± SD of separate series assays, each performed in triplicate. Inhibition constants (K_i) were calculated according to the equation of Cheng and Prusoff:[36] $K_i = IC_{50}/[1 + ([L]/K_d)]$, where [L] is the ligand concentration and K_d its dissociation constant. The K_d of [^{3}H]prazosin binding to rat cortex membranes was 0.24 nM (α_1), and the K_d of [^{3}H]rauwolscine binding to rat cortex membranes was 4 nM (α_2). [b] In parentheses are estimated and predicted affinity values calculated by Catalyst for the training set and test set, respectively. [c] Compounds used to build the test set. [d] Compounds used to build the training set. [e] Compounds described elsewhere by our research group.[17] [f] ND, not determined.

relevant conformations of the selected compounds (for example, atomic coordinates derived from X-ray crystallographic studies of their complexes with the putative receptor) are available, we resorted to a molecular mechanics approach to build the conformational models to be used for pharmacophore generation. All the conformers of each compound, within a range of 20 kcal/mol with respect to the global minimum, have been employed to derive a set of pharmacophore hypotheses.

Pharmacophore Description. As a result of pharmacophore generation, 100.9 bits as the total fixed cost (ideal hypothesis) and 154.9 bits as the cost of the null hypothesis have been found. The cost range over the 10 best generated hypotheses was 20.4 bits, suggesting that there was a homogeneous set of hypotheses and that the signal generated by this training set was strong. Moreover, the fact that the hypotheses were much closer to the fixed cost (i.e., the cost of hypothesis 1 is 112.9) meant that the signal could be interpreted.

The composition (in terms of chemical features that are necessary for activity), ranking score, and statistical parameters associated with the pharmacophore hypotheses are reported in Table 5. Even if the highest scoring hypothesis is usually the most likely to yield relevant information about the pharmacophore elements of a set of compounds, with the aim of extracting the maximum amount of information from the computational run, we have chosen to analyze the three highest-scoring hypotheses among the 10 pharmacophore models generated by the program.

Table 3. Chemical and Physical Data of the New Compounds

compd	X	*n*	formula	mp (°C)	yield (%)
3a	OCH_3	3	$C_{27}H_{33}ClN_6O_4$	183−185[a]	35
3b	Cl	3	$C_{26}H_{30}Cl_2N_6O_3$	95−100[b]	55
3c	OCH_3	2	$C_{26}H_{31}ClN_6O_4$	214−216[a]	70
3d	Cl	2	$C_{25}H_{28}Cl_2N_6O_3$	162−165[a]	35
3e	OCH_3	4	$C_{28}H_{35}ClN_6O_4$	106−110[b]	30
3f	Cl	4	$C_{27}H_{32}Cl_2N_6O_3$	228−230[b]	25
3g	OCH_3	5	$C_{29}H_{37}ClN_6O_4$	62−65[a]	60
3h	Cl	5	$C_{28}H_{34}Cl_2N_6O_3$	40−45[a]	60
3i	OCH_3	6	$C_{30}H_{39}ClN_6O_4$	96−98[b]	50
3j	Cl	6	$C_{29}H_{36}Cl_2N_6O_3$	70−75[b]	35
3k	OCH_3	7	$C_{31}H_{41}ClN_6O_4$	128−130[b]	70
3l	Cl	7	$C_{30}H_{38}Cl_2N_6O_3$	35−40[b]	65
4d	Cl	3	$C_{26}H_{31}ClN_6O_3$	102−105[b]	40
4e	OCH_3	4	$C_{28}H_{36}N_6O_4$	68−70[c]	20
4f	Cl	4	$C_{27}H_{33}ClN_6O_3$	35−40[b]	70
4g	OCH_3	5	$C_{29}H_{38}N_6O_4$	148−150[d]	45
4h	Cl	5	$C_{28}H_{35}ClN_6O_3$	48−52[d]	40
4i	OCH_3	6	$C_{30}H_{40}N_6O_4$	55−58[b]	65
4j	Cl	6	$C_{29}H_{37}ClN_6O_3$	70−74[c]	60
4k	OCH_3	7	$C_{31}H_{42}N_6O_4$	140−147[d]	50
4l	Cl	7	$C_{30}H_{39}ClN_6O_3$	75−78[b]	35
5	–	–	$C_{13}H_{13}ClN_4O_3$	214−216	40
7a	–	2	$C_{16}H_{18}BrClN_4O_3$	130−135	40
7b	–	4	$C_{18}H_{22}BrClN_4O_3$	oil	65
7c	–	5	$C_{15}H_{24}BrClN_4O_3$	oil	50
7d	–	6	$C_{16}H_{26}BrClN_4O_3$	oil	40
7e	–	7	$C_{17}H_{28}BrClN_4O_3$	oil	30
9a	–	4	$C_{17}H_{21}BrN_4O_3$	oil	50
9b	–	5	$C_{18}H_{23}BrN_4O_3$	oil	30
9c	–	6	$C_{18}H_{25}BrN_4O_3$	oil	30
9d	–	7	$C_{19}H_{27}BrN_4O_3$	oil	35

[a] As dihydrochloride monohydrate. [b] As dihydrochloride. [c] As trihydrochloride. [d] As trihydrochloride monohydrate.

All these three pharmacophores exhibit five chemical features and are characterized by either similar composition or spatial location of the features (Table 5). The major difference in composition arises from the replacement of one of the hydrophobic features found in both hypotheses 1 and 2 with a more specific aromatic ring feature (see Table 5 for the composition of hypothesis 3). Nevertheless, the RA-HY1 assembly (these two pharmacophore features were found at a 3.0 Å distance) of hypothesis 3 constitutes a constraint for the matching of the ligands with the pharmacophore. In fact, when the program tries to fit the substituted phenyl ring of the arylpiperazine moiety into the RA-HY1 system, the only possible orientation is that where RA is mapped by the phenyl group and HY1 by the methoxy substituent on the same ring. Thus, hypothesis 3 seems to be too restrictive with respect to the orientation of the substituted phenyl ring. Moreover, it was found to be characterized by a higher cost and rmsd, and by a lower correlation coefficient with respect to the first two hypotheses (Table 5). These findings, combined with the aim of broadening the possible orientations of the substituted phenyl moiety into the above-mentioned portion of the pharmacophore, led us to prefer hypotheses 1 and 2 over hypothesis 3. Hence, only hypotheses 1 and 2, bearing the HY1 and HY2 features (instead of RA and HY1 found in hypothesis 3) potentially mapped by either the phenyl ring or its substituent(s) in alternate conformations, were further investigated.

The vector describing HBA makes the difference between hypotheses 1 and 2. The three-dimensional

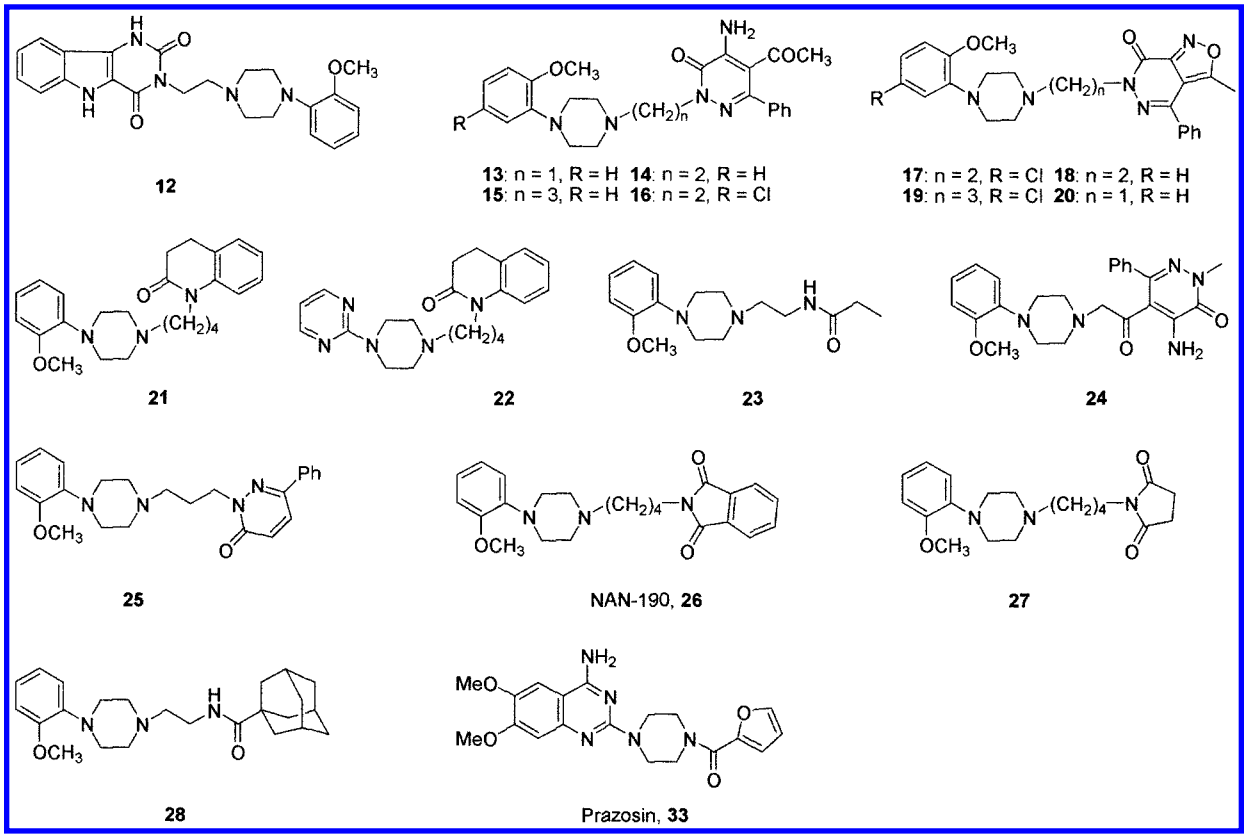

Figure 2. Structures of α_1-adrenoceptor antagonists collected from the literature.

Table 4. Actual and Calculated (Estimated or Predicted) α_1-Adrenergic Receptor Binding Affinities for Arylpiperazines Collected from the Literature, As Calculated by Catalyst

	K_i (nM)			K_i (nM)	
compd	actual	calcd	compd	actual	calcd
12[a,b]	0.21	0.11	**21**[a,b]	0.34	0.36
13[a,c]	2395	1200	**22**[a,b]	374	140
14[a,c]	24.6	15	**23**[a,b]	258	380
15[a,c]	46.7	11	**24**[a,c]	516	620
16[c,d]	42.7	11	**26**[b,d]	0.8	0.46
17[c,d]	15.6	9.2	**27**[b,d]	11.9	190
18[a,c]	147	68	**28**[b,d]	17.5	6.7
19[c,d]	7.9	0.86	**33**[d]	0.74	9.8 (1.1)[e]
20[a,c]	2308	1000			

[a] Compounds belonging to the training set. [b] Compounds taken from ref 22. [c] Compounds taken from ref 24. [d] Compounds belonging to the test set. [e] In parentheses is the affinity calculated using the manipulated pharmacophore model (see ref 31).

coordinates of the HBA projecting point (corresponding to the position of the hydrogen atom involved in hydrogen bonding with the hydrogen bond acceptor of the ligand) are in fact slightly different between the two hypotheses. On the basis of the very similar composition of the two hypotheses, hypothesis 1, characterized by the best statistical parameters (Table 5), has been chosen to represent "the pharmacophore model".

The regression line (Figure 3) of "true" versus "estimated" α_1-AR antagonist affinity for the training set, based on the lowest cost Catalyst-generated hypothesis, exhibited a correlation coefficient r of 0.92, and a root-mean-square deviation (rmsd) of 0.89. Comparison between the estimated affinity of the compounds in the training set relative to their experimentally measured values shows, in the worst case, a <7-fold difference and, in most cases, a <3-fold difference. These findings indicate a reliable ability to estimate the affinities of the training set. Moreover, the cost difference between hypothesis 1 and the null hypothesis is 42 bits, corresponding to an ~75% chance of true correlation in the data.

Figure 3 shows the five-feature hypothesis (characterized by three hydrophobic regions, a hydrogen bond acceptor, and a positive ionizable group) with compound **12**, the most active and small compound of the training set, superposed on it. The affinity of **12** is correctly estimated by the model, due to the fact that a complete mapping of the molecule onto the pharmacophore is possible. In detail, the tricyclic system fulfils both HY3 (with the phenyl group) and HBA (with the 1-carbonyl group of the six-membered heterocyclic ring). Both HY1 and HY2 are mapped by the *o*-methoxyphenyl moiety, and finally, the N-1 atom of the piperazine ring corresponds to the PI feature of the hypothesis. The strong antagonist effect of this molecule suggests that it possesses many or all of the molecular features required for activity. On the basis of the experimentally determined activity [0.21 nM (Table 3)] and taking into account the fact that the pharmacophore model correctly estimated the antagonist property of this compound [0.11 nM (Table 3)], one may conclude that all the pharmacophore features possibly account for the major interactions between antagonists and the receptor.

Compound **1c**, taken as a representative example of all pyridazinone derivatives, overlaps the pharmacophore model in a manner similar to that of **12**. In fact, the chemical functionalities of the hypothesis are all matched by the chemical groups of the ligand (Figure 5). Particularly, the arylpiperazinyl moiety maps the region where a cluster of features, known as crucial

Table 5. Composition (Features), Cost (Bits), and Statistical Parameters (rmsd and Correlation) Associated with the 10 Best Hypotheses (Pharmacophore Models)

hypothesis	feature 1[a]	feature 2[a]	feature 3[a]	feature 4[a]	feature 5[a]	cost[b]	rmsd	correlation
1	HBA	HY1	HY2	HY3	PI	112.9	0.89	0.92
2	HBA	HY1	HY2	HY3	PI	118.7	1.11	0.87
3	HBA	HY1	HY2	RA	PI	125.4	1.35	0.80
4	HBA	HY1	HY2	RA	PI	126.0	1.36	0.80
5	HBA	HY1	HY2	RA	PI	126.0	1.38	0.79
6	HBA	HY1	HY2	RA	PI	127.1	1.39	0.79
7	HBA	HY1	HY2	HY3	PI	127.5	1.43	0.78
8	HBA	HY1	HY2	HY3	PI	132.2	1.54	0.74
9	HBA	HY1	HY2	RA	PI	132.8	1.56	0.74
10	HBA	HY1	HY2	RA	PI	133.3	1.57	0.72

[a] HBA, hydrogen bond acceptor; HY, hydrophobic; PI, positive ionizable; RA, ring aromatic. [b] Expressed in bits.

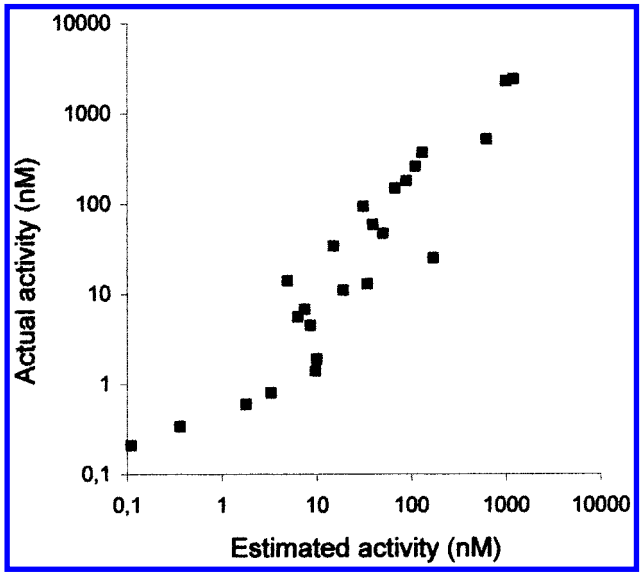

Figure 3. Regression line for hypothesis 1 (the pharmacophore model). The experimental vs estimated α_1-adrenoceptor binding affinity is reported for each member of the training set.

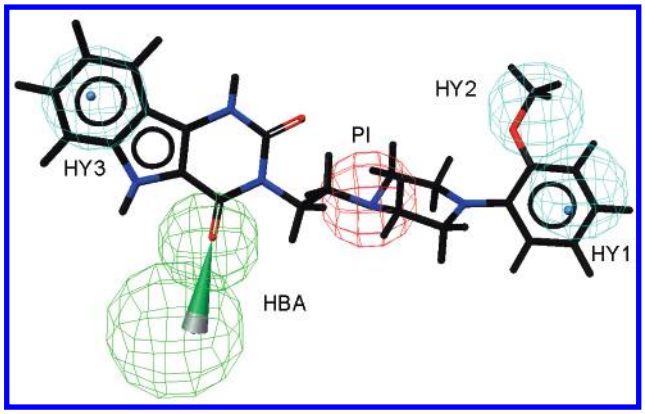

Figure 4. Compound **12**, the most active of the whole training set, mapped to the pharmacophore hypothesis. Pharmacophore features are color-coded: cyan for hydrophobic regions (HY1−HY3), green for a hydrogen bond acceptor (HBA), and red for a positive ionizable feature (PI).

elements for interacting with the putative receptor, lies. While the ortho-substituted phenyl ring (identified as A in the sketch reported in Scheme 2, and corresponding to the aromatic feature of the De Marinis pharmacophore model)[21] occupies both HY1 and HY2, the piperazinyl N-4 atom is located inside the positive ionizable feature PI, also identified by all the previously proposed pharmacophore models for α_1-AR antagonists. Among

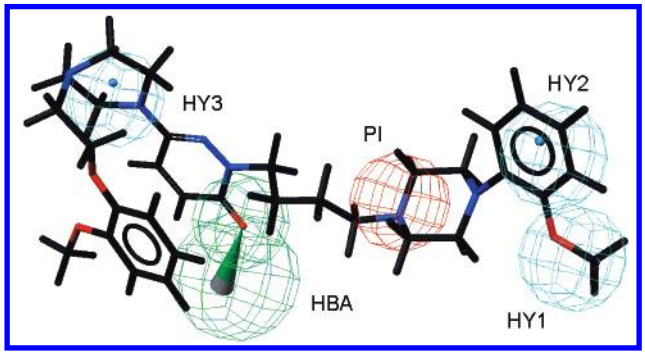

Figure 5. Compound **1c** mapped to the pharmacophore model. The sphere colors are described in the legend of Figure 4.

Scheme 2. Structures of Compounds **1**−**4**

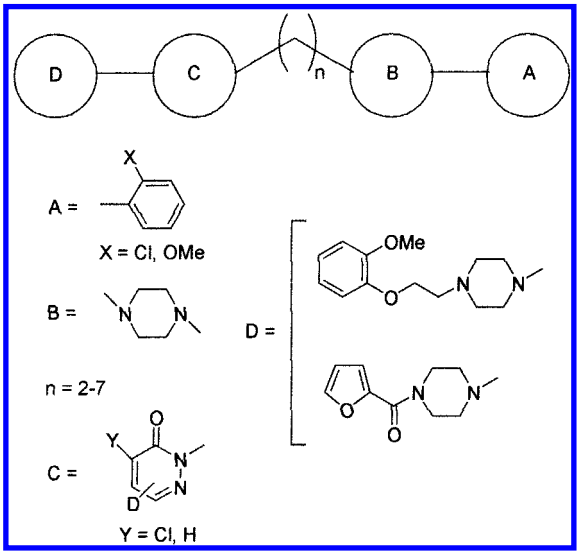

all the orientations of **1c** in the pharmacophore, it was found that the remaining two features (HBA and HY3) of the model are fulfilled by the ligand in two different ways. In most cases, while the carbonyl oxygen (or, sometimes, the N-1 atom) of the pyridazinone moiety (C in Scheme 2) overlaps the HBA feature (corresponding to the polar region in the De Marinis pharmacophore),[21] the piperazine directly bound to the pyridazinone ring reaches HY3 of the pharmacophore. Alternatively, the HY3 feature is sometimes mapped by the ortho substituent of the methoxyphenoxyethyl portion of the ligand.

From the analysis of the fitting mode of **1c** and other pyridazinone derivatives onto the best hypothesis, it turned out that this class of compounds is characterized by an "extra-size" portion of the molecule with respect

to **12** and other small compounds, exceeding the model itself. In the first orientation described above, the extra-size portion of **1c** is represented by the methoxyphenoxyethyl portion of the molecule (Figure 5), while in the second model, the exceeding moiety is the piperazinyl ring bound to the pyridazinone. Similar considerations can be made for compounds **3** and **4**. In fact, the furoyl moiety has been found to alternatively represent the chemical feature interacting with HY3 and the extra-size portion of the ligands. On the other hand, small and very active ligands have been found to perfectly overlap the pharmacophore model (Figure 4). As an additional example, the affinity of compound **25**, found to be ~1 order of magnitude more active than **4b**, **4c**, and **4e**,[17] has been predicted to be 5 nM, in good agreement with experimental data. In conclusion, it is possible that the exceeding moiety of the pyridazinone ligands **1**−**4** could represent a molecular portion able to contact particular regions of the receptor assigned to modulate the biological properties of these compounds.

The distance between the A−B and C−D portions of the ligand structures (Scheme 2) is influenced by the length of the polymethylene chain acting as a spacer linking B and C of pyridazinone derivatives **1**−**4**. Both the intrinsic high conformational flexibility of the Csp^3−Csp^3 polymethylene sequence and the length of the whole chain are crucial parameters influencing the goodness of fit of each compound to the chemical features of the pharmacophore model. In fact, while the PI, HY1, and HY2 features are mapped by most ligands, HBA and HY3 can be mapped only depending on the length of the polymethylene chain. In particular, $n = 2$ compounds are estimated to be weakly active due to the difficulty in mapping the HBA feature. This is in agreement with the experimental data of **1a**, **1g**, **2a**, **2h**, **3c**, and **4b**, the affinity values of each compound being the highest within the corresponding subset. Alternative orientations of compounds bearing the ethylene chain are characterized by an enhanced mapping to HBA, with the piperazinyl ring in B undergoing a deep conformational rearrangement leading to a very highly strained structure of the ligand.

The lengthening of the ethyl chain to a propyl spacer led to several compounds characterized by a higher conformational flexibility. This structural variation is responsible for the enhanced fit to the pharmacophore with a consequent improvement of the calculated affinity values. In fact, among compounds **1**−**4**, the propyl spacer-bearing derivatives are all more active than the corresponding ethylene analogues (Tables 1 and 2).

When $4 < n < 7$, by variation of dihedral angles of the polymethylene chain, the program is able to generate conformations of the most active ligands characterized by the optimum distance between the N-4 atom of the piperazine ring in B and the pyridazinone, allowing for a good overlapping to the features of the pharmacophore model. Thus, the distance between the A−B and C−D moieties of the ligands has been identified by the program as a key element in determining the goodness of fit to the pharmacophore features and, consequently, the estimated/predicted affinity values with respect to those experimentally determined. Moreover, molecules with slight structural differences are oriented by the program in a similar way into the pharmacophore, and any fluctuation of their affinity data is well accounted for on the basis of how well each compound overlays onto each of the pharmacophore features.

Finally, compounds characterized by an octyl spacer (**2g** and **2n**) exhibit a decreased affinity. We may interpret this observation by assuming that the conformation of the spacer, forced to bear the pyridazinone and piperazine rings at the PI−HBA distance, causes an intrachain steric hindrance between C-2 and C-6, thus reducing the overall affinity.

The substitution pattern on the phenyl ring of the arylpiperazine moiety is a crucial element for which to account with the purpose of rationalizing the relationships between the structural properties and affinities of the studied compounds. In particular, pharmacological tests highlighted the fact that the presence of a methoxy group or a chlorine atom at the ortho position of the arylpiperazine fragment is almost equivalent. In fact, while some subsets are characterized by decreased affinity corresponding to the presence of a chloride instead of a methoxy group (**2a**−**f** vs **2h**−**m**, **1e**,**f** vs **1k**,**l**, and **3g**,**i**,**k** vs **3h**,**j**,**l**), in the others the general trend goes in the opposite sense (**1a**−**d** vs **1g**−**j**, **3a**,**c**,**e** vs **3b**,**d**,**f**, and **4a**,**c**,**e**,**g**,**i**,**k** vs **4b**,**d**,**f**,**h**,**j**,**l**). The effect of a substitution of the phenyl ring is worthy of consideration also from the computational point of view. In particular, the *o*-methoxy group seems to be the optimum substituent that is able to interact with HY1 or HY2 of the pharmacophore model. Alternatively, an *o*-chloro or *m*-chloro (see compounds **16**, **17**, and **19**) substituent is also profitable for interaction with the model. In addition, HY1 or HY2 (depending on the orientation of the phenyl ring) is able to locate a hydrophobic group larger than a methoxy substituent (data not shown), according to the literature where *o*-isopropyl-substituted compounds with high α_1-AR affinity have been reported.[22]

From the above considerations, the three-dimensional structural properties required for an ideal α_1-antagonist can be summarized as follows. (i) A basic, positive ionizable nitrogen accessible to the receptor and easily protonable at physiological pH is required. This is the structural feature interacting with an aspartate side chain in the third transmembrane (TM) helix of the G-protein-coupled receptors (GPCRs). (ii) The ortho- or meta-substituted phenyl ring occupies both the HY1 and HY2 features of the pharmacophore, located 6.69 and 6.17 Å, respectively, from PI. In addition, the phenyl ring and each of its substituent can alternatively match HY1 or HY2 with a profitable fit value. These findings suggest that both HY1 and HY2 might constitute a unique and large hydrophobic pocket accommodating the ortho(meta)-substituted phenyl ring linked to the piperazine. (iii) A polar group (the pyridazinone ring in compounds **1**−**4**) at the other end of the molecule relative to the arylpiperazine moiety corresponds to a hydrogen bond acceptor (HBA, located 5.62 Å from PI) substituent. These results are in good agreement with the generally accepted statement that an α_1-AR antagonist interacts with the corresponding receptor by a three-pocket binding pathway;[21,23,24] while the most important structural element of the α_1-AR inhibitors is a protonated nitrogen atom interacting with the carboxylate group of an aspartic residue, the remaining

molecular portions of the ligand fit two binding pockets almost symmetrically located with respect to the aspartate. (iv) Finally, an additional hydrophobic pharmacophore element (HY3) accommodates (portions of) the terminal moieties linked to the pyridazinone. HY3 was found 9.78 Å from PI.

Pharmacophore Validation. (a) Fischer Test. Due to the relative small range between the cost for an ideal versus null hypothesis (54 bits), and due moreover to the small difference between the cost of hypothesis 1 and null hypothesis (42 bits), special care was taken to test the model for chance correlation. In fact, the 42 bits difference in the cost of the hypothesis representing the pharmacophore model and the null hypothesis can only ensure a 75% chance of true correlation. As a consequence, the pharmacophore model corresponding to hypothesis 1 was evaluated for the statistical significance using a randomization trial procedure derived from the Fischer method.[25] Experimental activities of the training set were scrambled 19 times to obtain spreadsheets with randomized activity data. Nineteen hypothesis generation experiments were performed using the scrambled training sets, and among the 190 resulting hypotheses (10 for each computational run), none was found with a lower cost than hypothesis 1. Thus, there was at least a 95% chance that hypothesis 1 represented true correlation in the data.

(b) Test Set. The validity and predictive power of hypothesis 1 were further assessed using molecules with known affinities for α_1-AR, outside the training set. This set of compounds (the test set) consists of pyridazinone derivatives and other compounds taken from the literature. According to the same guidelines that were followed to obtain the training set, the biological activities of compounds belonging to the test set have been determined as the ability to displace [^{3}H]prazosin from α_1 binding sites on rat cerebral cortex. The predicted affinities, calculated by Catalyst on the basis of the pharmacophore model, are reported in Tables 1, 2, and 4.

In particular, **17** is characterized by molecular fragments fulfilling all the features of the pharmacophore model. In fact, the 3-methyl and 7-carbonyl groups of the isoxazolo[3,4-*d*]pyridazin-7(6*H*)-one moiety map HY3 and HBA, respectively. Moreover, while the positive ionizable group PI is represented by the N-1 atom of the piperazine ring, the *m*-chlorophenyl substituent of the molecule corresponds to the HY1 and HY2 features of the model. It is interesting to note that the *o*-methoxy group, usually mapping to HY1 or HY2 in the pyridazinone derivatives, lies in an "empty" region of the space, due to the particular conformation assumed by the phenylpiperazine moiety. In fact, the piperazine ring is characterized by a N-1−N-4 diequatorial chair conformation with the plane of the C-2−C-3−C-5−C-6 system perfectly orthogonal to the phenyl ring. In this three-dimensional context, a conformation where the methoxy group is allowed to map one of the HY1 and HY2 hydrophobic features is forbidden because of steric clashes with the axial protons at both the C-2 and C-6 atoms of the piperazine. When some literature reporting an orthogonal conformation of the piperazine and the aryl ring as being highly profitable for the α_1-adrenoceptor affinity is considered,[22] alternative conformations of the piperazine ring and/or a different orientation of the substituted phenyl ring (i.e., allowing for a match on both HY1 and HY2, but leading to the lack of a fit into HY3) have been considered unprofitable and, then, investigated no further. The affinity of **17** for the α_1-AR has been predicted by the model to be 9.2 nM, in good agreement with the experimentally determined value of 15.6 nM.

Compound **18**, lacking the chlorine atom at the meta position on the phenyl ring, is characterized by an orientation into the pharmacophore model very similar to that of **17**. Also in this case, the three-dimensional features of the fitted conformers bearing the phenyl ring orthogonal to the piperazine plane, combined with the matching of the methyl group of the isoxazole ring into HY3, led to the impossibility of mapping the HY1 feature of the model. In fact, the program was unable to find any conformation characterized by the superposition of the *o*-methoxyphenyl moiety to both HY1 and HY2. As a consequence, the expected decrease in the antagonistic affinity of **18** with respect to **17** has been estimated with a value of 68 nM versus an actual affinity of 147.1 nM.

The lengthening of the polymethylene chain to a propyl moiety, combined with a twisted conformation of the piperazine ring, led to the complete mapping of **19** into the pharmacophore model. A reorientation of the phenyl group of **19** has been highlighted, the *o*-methoxyphenyl substituent assuming the usual orientation to fulfill both HY1 and HY2. As a consequence of this enhanced fit to the pharmacophore, the predicted affinity for **19** was 0.86 nM versus an actual value of 7.9 nM.

Finally, the shortening of the polymethylene chain to a methylene spacer led to a partial superposition of **20** onto the pharmacophore, the methyl group of the isoxazole ring being unable to reach HY3. Thus, the estimated affinity of **20** was 1000 nM versus an actual value of 2308 nM.

Compound **13**, the open analogue of **20**, fits into the model in an orientation similar to that of **20** and is also unable to map HY3. As a consequence, a poor affinity for **13** has been estimated by the program (1200 vs 2395 nM).

Estimated (**14** and **15**) or predicted (**16**) affinities (15, 11, and 11 nM, respectively) of the open analogues arise from how well each compound is able to fit into HY3 as a consequence of the transformation of the condensed isoxazole ring into both the 4-amino and 5-acetyl side chains on the pyridazinone ring. In fact, the conformational rigidity of the isoxazole ring serves as a constraint to orient the methyl group of **17**−**19** toward the HY3 feature of the pharmacophore. When the isoxazole was broken, the conformationally free acetyl side chain undergoes a conformational rearrangement to avoid steric clashes between its methyl group and the amino moiety at the 4-position. As a consequence, the measured dihedral angle between the plane passing through the acetyl moiety and the plane of the pyridazinone was ∼40°, only leading to a partial fit into HY3.

The phenyl ring directly linked to the pyridazinone moiety of compounds **13**−**20** failed to contact the pharmacophore model, due to the fact that this group is

located in the region of space where the extra-size portion of compounds **1**−**4** has been found.

A comparison of the estimated/predicted K_i values of **18** versus **14**, **17** versus **16**, and **19** versus **15** shows a good correlation with actual affinities. The affinity of **14**, where a good fit into HY1 was restored with respect to **18**, and a very partial fit into HY3 was found, has been estimated to be 15 nM instead an actual value of 24.6 nM. Moreover, decreased values calculated for **16** and **15** with respect to **17** and **19** derive from a partial mapping of HY3 by the methyl group of the acetyl moiety at the 5-position of the pyridazinone ring.

In summary, the pharmacophore model accounts for the trend in the biological data associated with compounds **17**−**20** and their open analogues **13**−**16**. Compounds with a methylene spacer (**20** and **13**) exhibit a markedly decreased antagonistic activity with respect to compounds with ethyl or propyl chains. This decrease is reflected in the estimated/predicted K_i values generated by means of our pharmacophore model where both **20** and **13** are completely unable to match the HY3 feature. Moreover, while compounds **14**−**16** are characterized by a partial fit to HY3, the conformational rigidity of **17**−**19** restores the ability of the methyl group of the isoxazole ring to locate itself within the HY3 feature of the pharmacophore model.

The model also accounts for the contribution of the terminal heterocyclic moiety (opposite the piperazine ring) to the affinity of each compound. As an example, compound **21**, whose terminal fragment linked through the polymethylene spacer to the piperazine ring is structurally different from that of **12** (estimated value of 0.11 nM vs an actual affinity of 0.21 nM), shows identical chemical features interacting with the pharmacophore. In particular, the condensed phenyl ring and the carbonyl group lie within HY3 and HBA, respectively, in a manner similar to that of the condensed phenyl ring and the 1-carbonyl group of **12**. PI, HY1, and HY2 are matched by the N-1 atom of the piperazine ring, and by the *o*-methoxyphenyl moiety, respectively. Compound **21** exhibits an estimated affinity of 0.36 nM versus an actual value of 0.34 nM. Compound **22**, bearing a pyrimidine ring instead of the *o*-methoxyphenyl substituent at the N-4 atom of the piperazine ring, is completely unable to map HY2. The model accounts for this modification with a predicted affinity of 140 nM versus an actual value of 374 nM.

In a similar way, the terminal fragment of NAN-190 (**26**, Figure 2), represented by a cyclic imide, possesses chemical substituents that are able to map both the HY3 and HBA features, with a predicted affinity of 0.46 nM versus an actual value of 0.8 nM. When the condensed phenyl ring was omitted, compound **27** (Figure 2), in the same orientation as **26**, cannot reach HY3, but one of the carbonyl groups is able to perfectly map HBA. As a consequence, the calculated affinity for this compound is 190 nM versus an actual value of 11.9 nM. Similarly, **23** is characterized by an ethyl spacer that is able to bring the carbonyl group of the aliphatic amide to interact with HBA, but the terminal ethyl group is far away from HY3 with a consequent predicted affinity of 380 nM versus an actual value of 258 nM. Compound **28** is predicted to have an affinity of 6.7 nM (17.5 nM is the actual value), mainly due to the adamantyl moiety (instead of the ethyl group of **23**) that is able to reach HY3.

As a summary of the validation step based on the prediction of affinity data for a set of compounds external to the training set, the pharmacophore model has accommodated much of the SAR for α_1-AR antagonists belonging to the arylpiperazine class. In fact, the importance of the ortho substituent has emerged, as well as the influence of the terminal heterocyclic moiety in defining the α_1-AR antagonist activity. Moreover, the distance between the arylpiperazine and the terminal fragment was demonstrated to be crucial for affinity.

(c) Database Search. With the purpose of further assessing the validity of the model, the five-feature pharmacophore model was used as a three-dimensional query to perform a database search to find other structural motifs that fulfill the functional and spatial constraints imposed by the model itself. The goal of this search was the identification of compounds previously reported in the literature and characterized by α_1-AR antagonist affinity. In particular, NCI (National Cancer Institute), Maybridge, MiniBioByte, and Sample databases (provided by MSI along with Catalyst 4.5), containing approximately 178 600 compounds, were searched using the pharmacophore model as a three-dimensional query and applying a molecular weight cutoff set to 700. As a result, 486 compounds (∼0.27% of the total) have been retrieved from the databases and investigated to find known α_1-AR antagonists. Within them, the pharmacophore model has identified compounds exhibiting α_1-AR affinity, and belonging to different structural classes with respect to that of the training set. As an example, the widely used antidepressant drug trazodone (2-{3-[4-(3-chlorophenyl)-1-piperazinyl]propyl}-1,2,4-triazolo[4,3-*a*]pyridin-3-one, **29**, Figure 6) has been recently reported to have an affinity of 281 nM (IC_{50} value) expressed as the ability to displace [^{3}H]prazosin from α_1-rat cortical membranes.[26] The affinity of **29** for α_1-AR has been predicted by the model to be 220 nM, with a partial mapping of the *m*-chlorophenyl moiety to HY1 and HY2, and a poor fit of the condensed pyridine ring to the HY3 feature.

Moreover, an open analogue of **29**, etoperidone (**30**, Figure 6),[27] characterized by an anti-α_1-adrenergic activity, has been also identified during the database search.

Several other compounds such as carpipramine (**31**, Figure 6)[28] and ergotamine (**32**, Figure 6),[29] reported to be blockers of α_1-adrenoceptors in the brain and at the periphery, respectively, have been also found in the databases.

Interestingly, prazosin (**33**, Figure 6), a compound with a very high affinity for α_1-AR, has been discarded because of its very poor fit to the pharmacophore hypothesis. This is due to the fact that the N-1 atom of the quinazoline ring has been drawn in the database as an unprotonated, uncharged atom. Thus, since Catalyst does not identify this atom as a positive ionizable feature, it tries to fit one of the nitrogen atoms of the piperazine ring to the PI feature of the pharmacophore model without finding any profitable mode of interaction. A previous study[30] highlighted the fact that the N-2 of prazosin is unlikely to be protonated, the

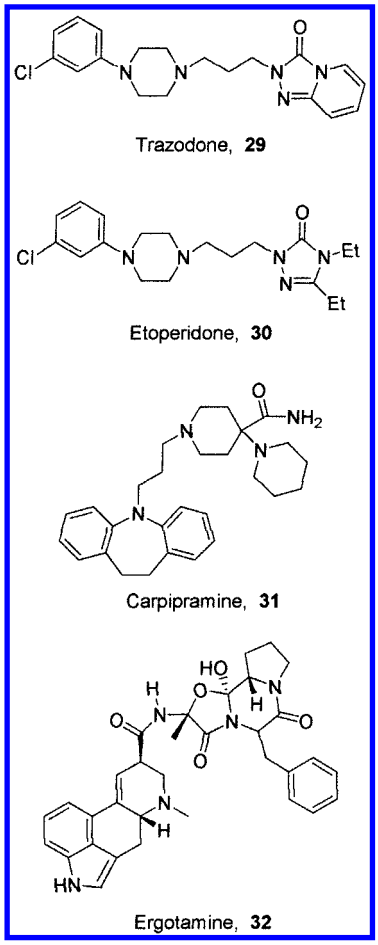

Figure 6. Structure of α_1-adrenoceptor antagonists identified using the pharmacophore model as a three-dimensional query in a database search.

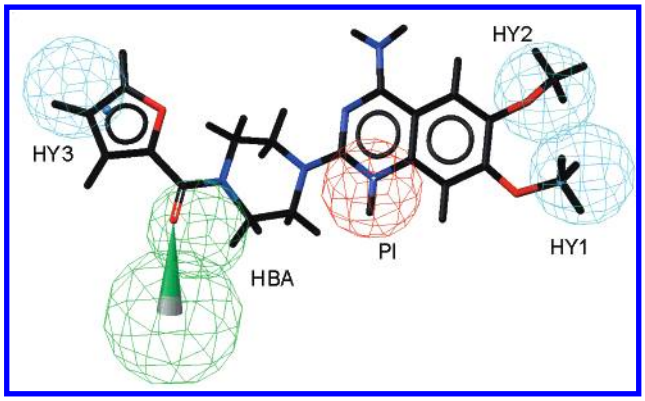

Figure 7. Prazosin (**33**) mapped to the pharmacophore model. The sphere colors are described in the legend of Figure 4.

energy difference for protonation at N-1 and N-2 being ~20 kcal/mol. In addition, the best superposition of N-1-protonated prazosin to the pharmacophore hypothesis led to a predicted affinity of 9.8 nM instead of the actual value of 0.74 nM.

The orientation of prazosin allows for a full matching of HY1 and HY2 with the methoxy substituents, the mapping of PI by the protonated nitrogen, the identification of the carbonyl oxygen as a HBA, and, finally, the partial mapping of HY3 by the C-4−C-5 portion of the furan ring (Figure 7).[31] Interestingly, the conformer used by the program to obtain the best superposition is characterized by the piperazine nitrogen atoms in a trigonal planar geometry, in accordance with a plausible conjugation effect of the piperazine nitrogens with both the quinazoline and furoyl moieties, and with X-ray crystallographic data reported in the Cambridge Structure Database[32] for *N*-arylpiperazine derivatives. In addition, the same structural features have been considered in recent three-dimensional QSAR studies of piperazines acting as α_1-AR and $5HT_{1A}$ antagonists.[20,33]

Results and Discussion

Tables 1 and 2 report the α_1- and α_2-adrenoceptor binding affinity, expressed as K_i values, of pyridazinone derivatives **1**−**4** containing an (ortho-substituted phenyl)piperazinylalkyl moiety.

Being aware that both the α_1- and α_2-AR are heterogenic species, but taking into account the fact that our major interest is the synthesis of selective α_1-AR antagonists (with respect to α_2-AR antagonists), we make the following comments about the structural features of compounds **1**−**4** that only refer to the native α_1- and α_2-adrenoceptors, and not to their relative subtypes.

From the binding data, it can be seen that most of these compounds demonstrated moderate to high affinity for α_1- and α_2-AR binding sites. Moreover, all the pyridazinone derivatives (**1**−**4**) exhibited higher affinity toward the α_1-AR than toward the α_2-AR, but poor α_2/α_1 selectivities. The only exception was found for compounds **1c** and **3k** with α_2/α_1 ratios corresponding to 103 and 274, respectively.

With respect to the phenylpiperazine substitution, compounds with a methoxy group at the ortho position display the best α_2/α_1 selectivity profile of the overall pyridazinone class, **1c** and **3k** being the most selective compounds.

The effect of the replacement of the *o*-methoxy group with a chlorine atom was difficult to rationalize. The introduction of a chlorine atom instead of the methoxy group led to a decreased affinity for the α_1-AR in several subsets (**2h**−**n**, **3h**,**j**,**l**, and **1k**,**l**). On the other hand, the opposite trend was found for compounds **3** and **4** bearing a furoyl moiety instead of the phenoxyethyl group. In fact, the affinities for the α_1-AR underwent an improvement by replacement of the methoxy with a chlorine group, with **3g**,**i**,**k** constituting an exception. Increased affinity was also observed for compounds **1a**−**d** with respect to chlorinate analogues **1g**−**j**. On the basis of these findings and taking into account reports[10,34] showing that the introduction of these two substituents (MeO and Cl) to the ortho position of the phenyl ring of the arylpiperazine chain may produce potent α_1-AR antagonists, we suggest that a methoxy or chlorine group is characterized by the same interaction pattern with the α_1-AR. These results are consistent with the molecular modeling studies showing either the methoxy or the chloro substituent interacting equally weighted with the same hydrophobic portion of the pharmacophore model built for α_1-AR antagonists. As a consequence, the diverse affinity for the α_1-AR highlighted for compounds **1**−**4** is mainly dependent on the terminal fragment linked through the spacer to the piperazine ring, and on the length of the polymethylene chain (the spacer) itself.

The length of the spacer linking the phenylpiperazine and pyridazinone moieties is of great importance for α_1

affinity and selectivity. As a general trend, the maximum affinity for both the α_1- and α_2-AR is reached with *n* ranging from 4 to 7. Reduction of the alkyl chain to *n* = 2 or 3 causes a relevant decrease in affinity in both receptors. This decrease is especially marked in derivatives bearing an ethylene or propylene spacer, for α_2 receptor binding.

The most active α_1-AR antagonists within the furoyl series are characterized by a five-carbon (**3g** and **3h**) or seven-carbon (**3k** and **4l**) atom spacer. An exception to these general observations was found in **3d** and **3b** where an ethylene or propylene spacer led to an affinity of 3.9 or 3.5 nM, respectively. On the other hand, in the phenoxyethyl series, the most active compounds are **1c** and **1i** (*n* = 4, 6-substituted pyridazinone), **2e** and **2l** (*n* = 6, 5-substituted pyridazinone), and, finally, **2f** and **2m** (*n* = 7, 5-substituted pyridazinone).

These findings led to the suggestion that the substitution pattern on the pyridazinone ring, combined with the extension of the alkyl spacer, had some relevant effects on the binding to the α-adrenoceptors. When a phenoxyethyl piperazine moiety is linked to the 5-position of the pyridazinone ring, a gradual increase in affinity was observed by lengthening the polymethylene chain up to a maximum of six (**2e** and **2l**) or seven (**2f** and **2m**) carbon atoms. On the contrary, the highest affinity for the 6-substituted pyridazinone derivatives has been found when the polymethylene chain is characterized by four carbon atoms (**1c** and **1i**).

Analogous considerations can be made for the series bearing a 1-(2-furoyl)piperazinyl fragment linked to the 5-position of the pyridazinone ring (compounds **3a**−**l**). A gradual increase in affinity was observed by lengthening the polymethylene spacer between the pyridazinone and arylpiperazine moieties of the molecule. While the highest affinity was found for compound **3g** (1.88 nM) characterized by a five-carbon alkyl chain and bearing a methoxy group at the ortho position of the phenylpiperazine fragment, the best selectivity is associated with compound **3k** (affinity of 1.95 nM, α_2/α_1 ratio of 274, seven-carbon alkyl chain). When the furoylpiperazine moiety is linked to the 6-position of the pyridazinone ring (compounds **4a**−**l**), a decreased affinity was observed toward α_1-AR with respect to 5-substituted pyridazinone derivatives **3a**−**l**. The highest affinity was observed with a six- or seven-carbon spacer. The chlorine atom at the ortho position of the arylpiperazine group led to an increased affinity with respect to a methoxy substituent.

We may interpret these observations by analyzing the fitting properties of each series to the pharmacophore model. In fact, the position of both HBA and PI constrained the spatial location of both the pyridazinone ring (whose carbonyl group was identified as the hydrogen bond acceptor feature of the pharmacophore for α_1-AR antagonists) and the N-1 atom of the piperazine moiety (the positive ionizable feature), at a defined distance. This distance constraint is well satisfied in most compounds as a consequence of the conformational freedom allowed by the polymethylene chain, and any fluctuation in affinity within the different series is the consequence of how well the compounds fit the most important pharmacophore elements around PI: HY1 and HY2 with the ortho-substituted phenyl ring and HBA with the pyridazinone. These three features (HBA, PI, and the HY1−HY2 assembly) constitute the minimum requirements for having α_1-AR antagonist activity, according to previously published literature. In addition, as reported above, different affinities also derived from variable matching to HY3 were considered as an additional pharmacophore feature with respect to the De Marinis model.[21]

These findings led to the conclusion that the substitution pattern on the pyridazinone ring influences the affinity, which is also strictly dependent on the polymethylene chain length.

Comparison between the Proposed Pharmacophore and Previously Published Models for α_1-AR. Recently published literature described the three-dimensional theoretical models of the complexes between compounds **13**−**20** and the three α_1-AR subtypes, as determined by molecular dynamics calculations. Having no structural information (i.e., distances between the key structural elements of these complexes) in our hands, we could make only qualitative comparisons between these structures and the pharmacophore model proposed in this paper. According to the DeMarinis α_1-AR model, each of the three complexes is characterized by three major binding subsites accommodating the inhibitors. In detail, an expected hydrogen bond between the basic nitrogen atom of the ligand and an aspartate lying in the third transmembrane domain (TM3) has been found. This interaction is also accounted for by the PI feature of our pharmacophore model. Moreover, an additional common structural feature is a hydrophobic pocket accommodating the substituted phenyl ring of the arylpiperazine moiety of inhibitors. This cavity is mainly formed by residues of TM4−TM6, and corresponds to both the HY1 and HY2 features of our pharmacophore model. Finally, a second binding pocket where, in turn, either the pyridazinone or the isoxazolopyridazinone moieties of the ligand lies, allows for different pathways of interaction with the inhibitor, for each of the three α_1-AR subtypes. In particular, a hydrogen bond involving both the carbonyl group of the pyridazinone moiety of the inhibitors and an arginine of TM7 has been evidenced in the DeBenedetti model for the α_{1D} subtype. The same interaction was also found in the pharmacophore model proposed by us, the carbonyl group of the pyridazinone ring of compounds **1**−**4** being the hydrogen bond acceptor.

Moreover, compounds **13**−**20**, some of which have been included in the hypothesis generation step, are generally characterized by an affinity for the α_{1D}-AR that is higher than that for both the α_{1A}- and α_{1B}-AR. In a similar way, evaluation of the α_1-AR subtype inhibitor properties for some of the compounds **1**−**4** (namely, **2a** and **4a**−**c**) showed affinity values for the α_{1D}- and α_{1A}-AR that were higher than that for α_{1B}-AR.

All these considerations led to the suggestion that the pharmacophore model proposed in this paper might incorporate the most relevant structural features of the α_{1D}-adrenoceptor, as suggested by a qualitative comparison with a theoretical model of the α_{1D}-AR reported in the recent literature. On the other hand, the pharmacophore model is distinguishable from that reported as the α_{1D}-AR model by, at least, two features. The first one is the inability to account for the interaction of the

phenyl ring directly linked to the pyridazinone with the receptor, reported as an important interaction key in determining the affinity for both α_{1A}- and α_{1D}-ARs. The second difference is related to the molecular portion corresponding to the isoxazole ring in compounds **17**−**20** or to the 4-acetyl and 5-amino side chains in compounds **13**−**16**. In fact, on the basis of how well these moieties can fit the HY3 feature, the pharmacophore model is able to account for different α_1-AR affinity values of compounds **13**−**20**. On the contrary, no discussion has been carried out on the isoxazole ring by DeBenedetti, probably because isoxazolopyridazinones **17**−**20** and trisubstituted pyridazinones **13**−**16** "give quite similar interaction patterns with each of the three α_1-AR subtypes".

Conclusions

We have prepared a new series of (ortho-substituted phenyl)piperazinylalkyl pyridazinone derivatives structurally related to previously described α_1- and α_2-AR antagonists. The pharmacophore model generation protocol provided by Catalyst has been successfully applied to some of these compounds to generate a three-dimensional model of the pharmacophore features responsible for α_1-AR antagonist activity. The resulting model provided significant correlation between the chemical structures of the studied compounds and their biological data. Some structural features of the pyridazinone derivatives have been demonstrated to be very important for the affinity and selectivity for the α_1-AR with respect to the α_2-AR. (i) The methoxy group at the ortho position of the phenylpiperazine moiety led to the best α_1 affinity−selectivity profile. In fact, two *o*-methoxyphenylpiperazinyl derivatives (namely, **1c** and **3k**) exhibited high affinity (0.6 and 1.9 nM, respectively) and interesting selectivity (103 and 274 as the α_2/α_1 ratios, respectively) values. These findings led to the conclusion that the ortho position could play a crucial role in the improvement of the α_1-AR antagonist properties in terms of affinity and selectivity. As a consequence, new substituents at the ortho position of the phenyl ring are currently under investigation. (ii) The polymethylene chain linking the arylpiperazine moiety to the pyridazinone ring is a critical structural feature in determining affinity and selectivity properties of compounds **1**−**4**. In fact, as demonstrated by modeling studies, the alkyl moiety serves as a spacer to bring both the pyridazinone and the arylpiperazine moiety to the optimal distance to interact with a hydrogen bond donor and a hydrophobic pocket of the putative receptor, respectively. This is in accordance with the De Marinis pharmacophore model, where an aromatic moiety is present instead of the more general hydrophobic pharmacophore feature of our model. (iii) Fitting of compounds bearing a long alkyl spacer to the computationally built pharmacophore model highlighted the fact that a portion of the polymethylene spacer or the terminal aromatic fragment (the phenoxyethyl or the furoyl moiety) could represent a portion of the molecule that is unable to interact with any pharmacophore feature. Moreover, the substitution pattern of the phenyl ring in the arylpiperazine moiety is worthy of further investigation. On the basis of these considerations, taking into account the fact that Catalyst does allow for pharmacophore generation based on the overall shape of the ligand, and on the basis of the use of a spatial region forbidden to the ligand (excluded volume features), we are currently carrying out some computational experiments to define the overall three-dimensional properties of the binding site for α_1-antagonists.

Experimental Section

Chemistry. Melting points were determined using a Kofler hot-stage apparatus and are uncorrected. ^{1}H NMR spectra were recorded on a Bruker AC 200 MHz instrument in the solvent indicated below. Chemical shift values (parts per million) are relative to tetramethylsilane used as an internal reference standard. Elemental analyses are within ±0.4% of theoretical values. Precoated Kiesegel 60 F_{254} plates (Merck) were used for TLC. The corresponding hydrochlorides were prepared by bubbling dry HCl into the dry solution of the compound.

Syntheses. Specific examples presented below illustrate general synthetic methods A−C.

4-Chloro-5-[4-(2-furoyl)piperazin-1-yl]pyridazin-3(2*H*)-one (5). A mixture of 4,5-dichloropyridazin-3(2*H*)-one (4.5 g, 27 mmol) and 1-(2-furoyl)piperazine (6.3 g, 27 mmol) in DMF in the presence of dry potassium carbonate was heated at reflux for 6 h. The same compound can be also obtained with refluxing ethanol and Et_3N for 20 h. The mixture was evaporated under reduced pressure and purified by chromatography on a silica gel column eluting with an EtOH/CH_2Cl_2 mixture (6:94) to give a 40% yield of an ivory solid: mp 214−216 °C; ^{1}H NMR ($CDCl_3$) δ 3.50−3.60 (m, 4H, H-pip), 3.90−4.10 (m, 4H, H-pip), 6.50 (dd, J = 1.7 and 3.4 Hz, 1H, H-fur), 7.10 (dd, J = 0.8 and 3.4 Hz, 1H, H-fur), 7.50 (dd, J = 0.8 and 1.7 Hz, 1H, H-fur), 7.70 (s, 1H, H6-pyrid), 12.00 (s, 1H, H2-pyrid).

2-(2-Bromoethyl)-4-chloro-5-[4-(2-furoyl)piperazin-1-yl]pyridazin-3(2*H*)-one (7a). This compound was prepared starting from **5** (3.08 g, 10 mmol) with 1,2-dibromoethane (5.63 g, 30 mmol) in benzene (50 mL). Potassium hydroxide pellets (5.61 g, 10 mmol) and tetrabutylammonium bromide (3.2 g, 10 mmol) were then added to the mixture, using the method reported by Yamada.[16] The residue was purified by chromatography on a silica gel column eluting with an EtOH/CH_2Cl_2 mixture (6:94) to give a 40% yield of a yellow solid: mp 130−135 °C; ^{1}H NMR ($CDCl_3$) δ 3.45−3.55 (m, 4H, H-pip), 3.75 (t, J = 7 Hz, 2H, CH_2), 3.90−4.00 (m, 4H, H-pip), 4.55 (t, J = 7 Hz, 2H, CH_2), 6.45 (dd, J = 1.7 and 3.4 Hz, 1H, H-fur), 7.00 (dd, J = 0.8 and 3.4 Hz, 1H, H-fur), 7.50 (dd, J = 0.8 and 1.7 Hz, 1H, H-fur), 7.60 (s, 1H, H-pyrid).

Method A Example. 2-{3-[4-(2-Methoxyphenyl)piperazin-1-yl]propyl}-4-chloro-5-[4-(2-furoyl)piperazin-1-yl]-pyridazin-3(2*H*)-one (3a). To 20 mL of dry ethanol were added sodium hydroxide (0.4 g, 10 mmol) and **5** (3.08 g, 10 mmol). This mixture was refluxed for 30 min, and then compound **6a** (2.68 g, 10 mmol) was summed up before dissolution in dry ethanol. The mixture was again refluxed under stirring for 15 h. After evaporation under reduced pressure, the residue was purified by chromatography on a silica gel column eluting with an EtOH/CH_2Cl_2 mixture (5:95) to give a 35% yield of a dense oil: ^{1}H NMR ($CDCl_3$) δ 2.10 (quint, J = 7 Hz, 2H, CH_2), 2.50 (t, J = 7 Hz, 2H, CH_2), 2.65−2.80 (m, 4H, H-pip), 3.10−3.20 (m, 4H, H-pip), 3.40−3.50 (m, 4H, H-pip), 3.85 (s, 3H, OCH_3), 3.95−4.10 (m, 4H, H-pip), 4.25 (t, J = 7 Hz, 2H, CH_2), 6.50 (dd, J = 1.7 and 3.4 Hz, 1H, H-fur), 6.80−7.00 (m, 4H, H-arom), 7.10 (dd, J = 0.8 and 3.4 Hz, 1H, H-fur), 7.50 (dd, J = 0.8 and 1.7 Hz, 1H, H-fur), 7.60 (s, 1H, H-pyrid). For the corresponding hydrochloride: mp 183−185 °C. Anal. ($C_{27}H_{33}ClN_6O_4 \cdot 2HCl \cdot H_2O$) C, H, N.

Method B Example. 2-{4-[4-(2-Methoxyphenyl)piperazin-1-yl]butyl}-6-[4-(2-furoyl)piperazin-1-yl]pyridazin-3(2*H*)-one (4e). This compound was obtained from **11a** with 1-(2-methoxyphenyl)piperazine in isoamyl alcohol and dry sodium carbonate. **4e** was purified by cromatography on a silica gel column eluted with an EtOH/CH_2Cl_2 mixture (11:89) to give a 20% yield of a dense oil: ^{1}H NMR ($CDCl_3$) δ 1.70−

1.90 (m, 4H, $2CH_2$), 2.60−2.80 (m, 2H, CH_2), 2.90−3.00 (m, 4H, H-pip), 3.10−3.40 (m, 8H, H-pip), 3.85 (s, 3H, OCH_3), 3.95−4.00 (m, 4H, H-pip), 4.10 (t, J = 7 Hz, 2H, CH_2), 6.50 (dd, J = 1.7 and 3.4 Hz, 1H, H-fur), 6.80−7.05 (m, 6H, 4H-arom, 1H-pyrid, 1H-fur), 7.15 (d, J = 9 Hz, 1H, H-pyrid), 7.50 (dd, J = 0.8 and 1.7 Hz, 1H, H-fur). For the corresponding hydrochloride: mp 68−70 °C. Anal. ($C_{28}H_{36}N_6O_4 \cdot 3HCl$) C, H, N.

Method C Example. 2-(4-Bromobutyl)-4-chloro-5-[4-(2-furoyl)piperazin-1-yl]pyridazin-3(2*H*)-one (7b). A mixture of **5** (6.2 g, 20 mmol) with 1,4-dibromobutane (5.1 g, 30 mmol) and dry potassium carbonate (4.1 g, 30 mmol) in 50 mL of acetone was refluxed under stirring for 20 h. The filtered residue was evaporated under reduced pressure and purified by chromatography on a silica gel column eluting with an $EtOH/CH_2Cl_2$ mixture (5:95) to give a 65% yield of a dense oil: ^{1}H NMR ($CDCl_3$) δ 1.60−2.00 (m, 4H, $2CH_2$), 3.30−3.55 (m, 6H, H-pip, CH_2), 3.80−3.90 (m, 4H, H-pip), 4.15 (t, J = 7 Hz, 2H, CH_2), 6.45 (dd, J = 1.7 and 3.4 Hz, 1H, H-fur), 7.00 (dd, J = 0.8 and 3.4 Hz, 1H, H-fur), 7.50 (dd, J = 0.8 and 1.7 Hz, 1H, H-fur), 7.60 (s, 1H, H-pyrid).

Radioligand Binding Assays. The pharmacological profile of compounds **1**−**4** was evaluated for their affinities for α_1- and α_2-adrenoceptors by determining for each compound its ability to displace [^{3}H]prazosin or [^{3}H]rauwolscine from specific binding sites on rat cerebral cortex. K_i values were determined on the basis of three competition binding experiments in which seven drug concentrations, run in triplicate, were used.

α_1-Receptor Binding. Rat cerebral cortex was homogenized in 20 volumes of ice-cold 50 mM Tris-HCl buffer at pH 7.7 containing 5 mM EDTA (buffer T_1) in an ultra-turrax homogenizer. The homogenate was centrifuged at 48000*g* for 15 min at 4 °C. The pellet (P_1) was suspended in 20 volumes of ice-cold buffer T_1. It was then homogenized and centrifuged at 48000*g* for 15 min at 4 °C. The resulting pellet (P_2) was frozen at −80 °C until the time of assay.

Pellet P_2 was suspended in 20 volumes of ice-cold 50 mM Tris-HCl buffer at pH 7.7 (T_2 buffer), and the α_1 binding assay was performed in triplicate by incubating at 25 °C for 60 min in 1 mL of T_2 buffer containing aliquots of the membrane fraction (0.2−0.3 mg of protein) and 0.1 nM [^{3}H]prazosin in the absence or presence of unlabeled 1 μM prazosin. The binding reaction was terminated by filtering through Whatman GF/C glass fiber filters under suction and washing twice with 5 mL of ice-cold Tris buffer. The filters were placed in scintillation vials, and 4 mL of Ultima Gold MN Cocktail solvent scintillation fluid (Packard) was added. The radioactivity was assessed with a Packard 1600 TR scintillation counter. The level of specific binding was obtained by subtracting the level of nonspecific binding from the total level of binding and was approximated to be 85−90% of the total level of binding.

α_2-Receptor Binding. Cerebral cortex was dissected from rat brain, and the tissue was homogenized in 20 volumes of ice-cold 50 mM Tris-HCl buffer at pH 7.7 containing 5 mM EDTA, as reported above (buffer T_1). The homogenate was centrifuged at 48000*g* for 15 min at 4 °C. The resulting pellet was diluted in 20 volumes of 50 mM Tris-HCl buffer at pH 7.7 and used in the binding assay.

The binding assay was perfomed in triplicate, by incubating aliquots of the membrane fraction (0.2−0.3 mg of protein) in Tris-HCl buffer at pH 7.7 with approximately 2 nM [^{3}H]-rauwolscine in a final volume of 1 mL. Incubation was carried out at 25 °C for 60 min. Nonspecific binding was defined in the presence of 10 μM rauwolscine. The binding reaction was concluded by filtration through Whatman GF/C glass fiber filters under reduced pressure. Filters were washed four times with 5 mL aliquots of ice-cold buffer and placed in scintillation vials. The level of specific binding was obtained by subtracting the level of nonspecific binding from the total level of binding and approximated to be 85−90% of the total level of binding. The receptor-bound radioactivity was assessed as described above.

Compounds were dissolved in buffer or DMSO (2% buffer concentration) and added to the assay mixture. A blank experiment was carried out to determine the effect of the solvent on binding. Protein estimation was based on a reported method,[35] after solubilization with 0.75 N sodium hydroxide, using bovine serum albumin as a standard. The concentration of tested compound that produces 50% inhibition of specific [^{3}H]prazosin or [^{3}H]rauwolscine binding (IC_{50}) was determined by log-probit analysis with seven concentrations of the displacer, each performed in triplicate. Inhibition constants (K_i) were calculated according to the equation[36] $K_i = IC_{50}/[1 + ([L]/K_d)]$, where [L] is the ligand concentration and K_d its dissociation constant. The K_d for [^{3}H]prazosin binding to cortex membranes was 0.24 nM (α_1), and the K_d for [^{3}H]rauwolscine binding to cortex membranes was 4 nM (α_2).

Computational Methods. All calculations and graphic manipulations were performed on a Silicon Graphics O2 workstation by means of the Catalyst 4.5 software package. Fourteen compounds belonging to a new class of pyridazinone derivatives (Tables 1 and 2) and 10 additional compounds taken from the literature (namely, compounds **12**−**15**, **18**, and **20**−**24**, reported in Figure 2), all characterized by α_1-AR antagonistic activity, have been used in this study to build a 24-compound training set.

All the compounds of the training and test set were built using the two- and three-dimensional sketcher of the program. A representative family of conformations were generated for each molecule using the poling algorithm and the "best quality conformational analysis" method[37] (CHARMm force field).[38,39]

The "best quality" is considered as the method of choice also for systems with flexible rings. In this context, among Catalyst users, this conformational search procedure seems to have caused some problems about the axial/equatorial distribution of substituents in satured six-membered rings.[40] In addition, distorted molecular geometries have been occasionally found.[40] In our case, almost a balanced distribution of axial and equatorial (representing the most favorable conformations) substituents on the piperazine ring was highlighted. Moreover, the structures of the generated conformers showed a quasi-coplanar orientation of the piperazine ring with respect to the pyridazinone moiety directly linked to it, in agreement with some literature reports for piperazine derivatives.[20] In addition, twisted or even orthogonal conformations of the piperazine with respect to the phenyl ring of the arylpiperazinyl moiety of the ligands, demonstrated to be highly profitable for α_1-AR antagonism, were also found.[22]

Conformational diversity was emphasized by selection of the conformers that fell within the 20 kcal/mol range above the lowest-energy conformation that was found.

The training set of molecules, with their associated conformational models, were submitted to Catalyst hypothesis generation with the aim of building potential pharmacophore models. The chemical functions used in this generation step are only surface-accessible features (i.e., the environment around the feature is sufficiently uncrowded). In particular, hydrogen bond acceptor lipid (HBA), hydrogen bond donor (HBD), positive ionizable (PI), ring aromatic (RA), and hydrophobic (HY) features[41] have been included in the calculations. Hydrogen bond acceptor lipid includes basic nitrogen not considered in the hydrogen bond acceptor feature.

A couple of constraints have been imposed on the hypothesis generator. (i) Only hypotheses with five features have been kept because of the molecular flexibility and functional complexity of the training set. (ii) On the basis of the literature reporting a positive ionizable group as a critical key for antagonistic activity,[23,30,42,43] the program was forced to include such a feature in the composition of hypotheses.

A database search has been performed using the "best flexible search" method provided by Catalyst. It is allowed to flex the conformational models stored in the databases to map the three-dimensional query represented by the pharmacophore hypothesis (hypothesis 1). Only molecules mapping all the features of the hypothesis were considered as hits. A total of 486 compounds were identified and ranked by descending predicted affinities for the α_1-AR.

Acknowledgment. Financial support provided by the Italian "Ministero dell'Università e della Ricerca Scientifica e Tecnologica" (MURST), and Italian Research National Council (CNR) "Progetto Finalizzato Biotecnologie" (CNR Target Project on "Biotechnology) is acknowledged.

References

(1) A portion of this research was presented at the XVIth International Symposium on Medicinal Chemistry, Bologna, Italy, September 18−22, 2000 (Abstract PC-14).

(2) (a) Ford, A. P. D. W.; Williams, T. J.; Blue, D. R.; Clarke, D. E. α_1-Adrenoceptor Classification: Sharpening Occam's Razor. *Trends Pharmacol. Sci.* **1994**, *15*, 167−170. (b) Hieble, J. P.; Bylund, D. B.; Clarke, A. E.; Eikenberg, D. C.; Langer, S. Z.; Lefkowitz, R. J.; Minneman, K. P.; Ruffolo, R. R., Jr. International Union of Pharmacology X. Recommendation for Nomenclature of α_1-Adrenoceptors: Consensus Update. *Pharmacol. Rev.* **1995**, *47*, 266−270. (c) Hieble, J. P.; Ruffolo, R. R., Jr. Subclassification and Nomenclature of α_1- and α_2-Adrenoceptors. *Prog. Drug Res.* **1996**, *47*, 81−130.

(3) Price, D. T.; Schwinn, D. A.; Lomasney, J. W.; Allen, L. F.; Caron, M. G.; Lefkowitz, R. J. Identification, Quantitation, and Localization of mRNA for Three Distinct α_1 Adrenergic Subtypes in Human Prostate. *J. Urol.* **1993**, *250*, 546−551.

(4) Lepor, H. The Emerging Role of Alpha Antagonists in the Therapy of Benign Prostatic Hyperplasia. *J. Androl.* **1991**, *12*, 389−394.

(5) Caine, M. Alpha-Adrenergic Blockers for the Treatment of Benign Prostatic Hyperplasia. *Urol. Clin. North Am.* **1990**, *17*, 641−649.

(6) Gifford, R. W., Jr. The fifth report of the Joint National Committee on Detection, Evaluation, and Treatment of High Blood Pressure: Insights and Highlights from the Chairman. *Cleveland Clinic Journal of Medicine* **1993**, *60*, 273−277.

(7) Ames, R. P.; Kiyasu, J. Y. α_1-Adrenoceptor Blockade with Doxazosin in Hypertension: Effects on Blood Pressure and Lipoproteins. *J. Clin. Pharmacol.* **1989**, *29*, 123−127.

(8) Strader, C. D.; Sigal, I. S.; Dixon, R. A. Structural Basis of β-Adrenergic Receptor Function. *FASEB J.* **1989**, *3*, 1825−1832.

(9) Strader, C. D.; Sigal, I. S.; Dixon, R. A. Genetic Approaches to the Determination of Structure−Function Relationships of G Protein-Coupled Receptors. *Trends Pharmacol. Sci.* **1989** (Dec. Suppl.), 26−30.

(10) Russo, F.; Romeo, G.; Guccione, S.; De Blasi, A. Pyrimido[5,4-*b*]indole derivatives. 1. A new Class of Potent and Selective α_1 Adrenoceptor Ligands. *J. Med. Chem.* **1991**, *34*, 1850−1854.

(11) Jaszlits, L.; Rabloczky, G.; Csokas, G.; Bodi, I.; Kurthy, M.; Horvath, E.; Kovacs, A.; Jednakovits, A.; Aranyi, P.; Matyus, P. GYKI-12 743, a Novel Antihypertensive Compound with Special α-Adrenergic Blocking Profile. *Acta Physiol. Hung.* **1990**, *75* (Suppl.), 155−156.

(12) Corsano, S.; Strappaghetti, G.; Barbaro, R.; Giannaccini, G.; Betti, L.; Lucacchini, A. Synthesis of New Pyridazinone Derivatives and their Affinity Towards α_1-α_2-Adrenoceptors. *Bioorg. Med. Chem.* **1999**, *7*, 933−941.

(13) *Catalyst 4.5*; Molecular Simulations, Inc.: San Diego.

(14) Gomez-Gil, M. C.; Gomez-Parra, V.; Sanchez, F.; Torres, T. 4,5-Disubstituted Pyridazin-3(2*H*)-ones as Hypotensive Drugs: Incorporation of a β-Blocking Moiety. *Arch. Pharm.* **1986**, *319*, 60−64.

(15) Bourdais, J. Alkylation of Piperazine in N,N-Dimethylformamide. *Bull. Soc. Chim. Fr.* **1968**, *8*, 3246−3249.

(16) Yamada, T.; Tsukamoto, Y.; Shimamura, H.; Banno, S.; Sapo, M. *Eur. J. Med. Chem.* **1983**, *18*, 209−214.

(17) Corsano, S.; Strappaghetti, G.; Leonardi, A.; Rhazri, K.; Barbaro, R. New 3(2*H*)-Pyridazinone Derivatives: Synthesis and Affinity Towards α_1AR Subtypes and 5HT$_{1A}$ Receptors. *Eur. J. Med. Chem.* **1997**, *32*, 339−342.

(18) The rules for picking training sets are reported at http://www.msi.com/support/catalyst/hypogen.html.

(19) Lopez-Rodriguez, M. L.; Rosado, M. L.; Benhamu, B.; Morcillo, M. J.; Fernandez, E.; Schaper, K.-J. Synthesis and Structure−Activity Relationships of a New Model of Arylpiperazines. 2. Three-Dimensional Quantitative Structure−Activity Relationships of Hydantoin-Phenylpiperazine Derivatives with Affinity for 5-HT$_{1A}$ and α_1 Receptors. A Comparison of CoMFA Models. *J. Med. Chem.* **1997**, *40*, 1648−1656.

(20) Cinone, N.; Carrieri, A.; Strappaghetti, G.; Corsano, S.; Barbaro, R.; Carotti, A. Comparative Molecular Field Analysis of Some Pyridazinone-containing α_1-Antagonists. *Bioorg. Med. Chem.* **1999**, *7*, 2615−2620.

(21) De Marinis, R. M.; Wise, M.; Hieble, J. P.; Ruffolo, R. R., Jr. Structure−Activity Relationships for α-1 Adrenergic Receptor Agonists and Antagonists. In *The Alpha-1 Adrenergic Receptor*; Ruffolo, R. R., Jr., Ed.; Humana Press: Clifton, NJ, 1987; pp 211−265.

(22) Mokrosz, M. J.; Paluchowska, M. H.; Charakchieva-Minol, S.; Bien, S. Effect of Structural Modifications in 1-Arylpiperazine Derivatives on α_1-Adrenoceptor Affinity. *Arch. Pharm. Pharm. Med. Chem.* **1997**, *330*, 177−180.

(23) (a) Bremner, J. B.; Coban, B.; Griffith, R. Pharmacophore Development for Antagonists at α_1 Adrenergic Receptor Subtypes. *J. Comput.-Aided Mol. Des.* **1996**, *10*, 545−557. (b) Griffith, R.; Bremner, J. B. Modelling of Adrenoceptor Ligand Targets Based on Novel Medium- or Macro-sized Fused Nitrogen Heterocyclic Systems. *J. Comput.-Aided Mol. Des.* **1999**, *13*, 69−78. (c) Bremner, J. B.; Coban, B.; Griffith, R.; Groenewoud, K. M.; Yates, B. F. Ligand Design for α_1 Adrenoceptor Subtype Selective Antagonists. *Bioorg. Med. Chem.* **2000**, *8*, 201−214.

(24) Montesano, F.; Barlocco, D.; Dal Piaz, V.; Leonardi, A.; Poggesi, E.; Fanelli, F.; De Benedetti, P. G. Isoxazolo-[3,4-*d*]-pyridazin-7-(6*H*)-ones and their Corresponding 4,5-Disubstituted-3-(2*H*)-pyridazinone Analogues as New Substrates for α_1-Adrenoceptor Selective Antagonists: Synthesis, Modeling, and Binding Studies. *Bioorg. Med. Chem.* **1998**, *6*, 925−935.

(25) Fischer, R. The Principle of Experimentation, Illustrated by a Psycho-Physical Experiment. In *The Design of Experiments*; Hafner Publishing Co.: New York, 1966; Chapter II.

(26) Giannangeli, M.; Cazzolla, N.; Luparini, M. R.; Magnani, M.; Mabilia, M.; Picconi, G.; Tomaselli, M.; Baiocchi, L. Effect of Modification of the Alkylpiperazine Moiety of Trazodone on 5HT$_{2A}$ and α_1 Receptor Binding Activity. *J. Med. Chem.* **1999**, *42*, 336−345.

(27) Costa, A.; Martignoni, E.; Blandini, F.; Petraglia, F.; Genazzani, A. R.; Nappi, G. Effects of Etoperidone on Sympathetic and Pituitary-adrenal Responses to Diverse Stressors in Humans. *Clin. Neuropharmacol.* **1993**, *16*, 127−138.

(28) Setoguchi, M.; Sakamori, M.; Takehara, S.; Fukuda, T. Effects of Iminodibenzyl Antipsychotic Drugs on Cerebral Dopamine and Alpha-adrenergic Receptors. *Eur. J. Pharmacol.* **1985**, *112*, 313−322.

(29) (a) Roquebert, J.; Grenie, B. Alpha 2-Adrenergic Agonist and Alpha 1-Adrenergic Antagonist Activity of Ergotamine and Dihydroergotamine in Rats. *Arch. Int. Pharmacodyn. Ther.* **1986**, *284*, 30−37. (b) Bonuso, S.; Di Stasio, E.; Marano, E.; Covelli, V.; Testa, N.; Tetto, A.; Buscaino, G. A. The Antimigraine Effect of Ergotamine: a Role for Alpha-adrenergic Blockade? *Acta Neurol.* **1994**, *16*, 1−10.

(30) De Benedetti, P. G.; Menziani, M. C.; Rastelli, G.; Cocchi, M. Molecular Orbital Study of the Nitrogen Basicity of Prazosin Analogues in Relation to their α_1-Adrenoceptor Binding Affinity. *THEOCHEM* **1991**, *233*, 343−351.

(31) Considering the 13-fold difference in the predicted/actual affinity of prazosin **29**, mainly due to a partial mapping into HY3, we have increased by 0.5 Å the radius of the sphere representing this hydrophobic feature. As a result, an improved fit (from 9.0 to 10.4) and a predicted affinity value of 1.1 nM, in good agreement with the experimental data (0.74 nM), were found. Although this finding is to be considered as a preliminary result, it suggested that a hydrophobic region larger than HY3 might improve the goodness of ligand affinity versus the receptor. Evaluation of the influence of the HY3 size on the affinity is currently under investigation.

(32) Allen, F. H.; Kennard, O. 3D Search and Research Using the Cambridge Structural Database. *Chem. Des. Autom. News* **1993**, *8*, 31−37.

(33) Gaillard, P.; Carrupt, P. A.; Testa, B.; Schambel, P. Binding of Arylpiperazines, (Aryloxy)propanolamines, and Tetrahydropyridylindoles to the 5-HT$_{1A}$ Receptor: Contribution of the Molecular Lipophilicity Potential to Three-Dimensional Quantitative Structure-Affinity Relationship Models. *J. Med. Chem.* **1996**, *39*, 126−134.

(34) Chern, J.-W.; Yen, M.-H.; Lu, G.-Y.; Shiau, C.-Y.; Lai, Y.-J.; Chan, C.-H. Studies on Quinazoline. 5. 2,3-Dihydroimidazo[1,2-*c*]quinazoline Derivatives: A Novel Class of Potent and Selective α_1-Adrenoceptor Antagonists and Antihypertensive Agents. *J. Med. Chem.* **1993**, *36*, 2196−2207.

(35) Lowry, O. H.; Rosenbrough, N. J.; Farr, A. L.; Randall, R. J. Protein Measurement with the Folin Phenol Reagent. *J. Biol. Chem.* **1951**, *193*, 265−275.

(36) Cheng, Y. C.; Prusoff, W. H. Relationship between the Inhibition Constant (K_i) and the Concentration of Inhibitor which Causes 50% Inhibition (IC$_{50}$) of an Enzymatic Reaction. *Biochem. Pharmacol.* **1973**, *22*, 3099−3108.

(37) (a) Smellie, A.; Teig, S. L.; Towbin, P. Poling: Promoting Conformational Coverage. *J. Comput. Chem.* **1995**, *16*, 171−187. (b) Smellie, A.; Kahn, S. D.; Teig, S. L. An Analysis of Conformational Coverage 1. Validation and Estimation of Coverage.

J. Chem. Inf. Comput. Sci. **1995**, *35*, 285−294. (c) Smellie, A.; Kahn, S. D.; Teig, S. L. An Analysis of Conformational Coverage 2. Applications of Conformational Models. *J. Chem. Inf. Comput. Sci.* **1995**, *35*, 295−304.

(38) Brooks, B. R.; Bruccoleri, R. E.; Olafson, B. D.; States, D. J.; Swaminathan, S.; Karplus, M. CHARMm: A Program for Macromolecular Energy, Minimization, and Dynamics Calculations. *J. Comput. Chem.* **1983**, *4*, 187, 217.

(39) Catalyst force field and potential energy functions are described in the file REFenergy.doc.html provided by MSI along with the program Catalyst 4.5.

(40) Further information is available at the Catalyst mailing list (http://www.msi.com/user/groups/catalyst/cat-archive-dir/index.html) under the subject "Catalyst 4.5 conformations".

(41) Greene, J.; Kahn, S. D.; Savoj, H.; Sprague, P.; Teig, S. L. Chemical Function Queries for 3D Database Search. *J. Chem. Inf. Comput. Sci.* **1994**, *34*, 1297−1308.

(42) De Benedetti, P. G.; Cocchi, M.; Menziani, M. C.; Fanelli, F. Theoretical Quantitative Size and Shape Activity Selectivity Analyses of 5-HT_{1A} Serotonin and α-Adrenergic Receptor Ligands. *J. Mol. Struct.* **1994**, *305*, 101−110.

(43) Cocchi, M.; Fanelli, F.; Menziani, M. C.; De Benedetti, P. G. Theoretical Quantitative Structure−Activity Relationship Analysis of Congeneric and Non-Congeneric 1-Adrenoceptor Antagonists: a Chemometric Study. *J. Mol. Struct.* **1995**, *331*, 79−93.

JM010821U